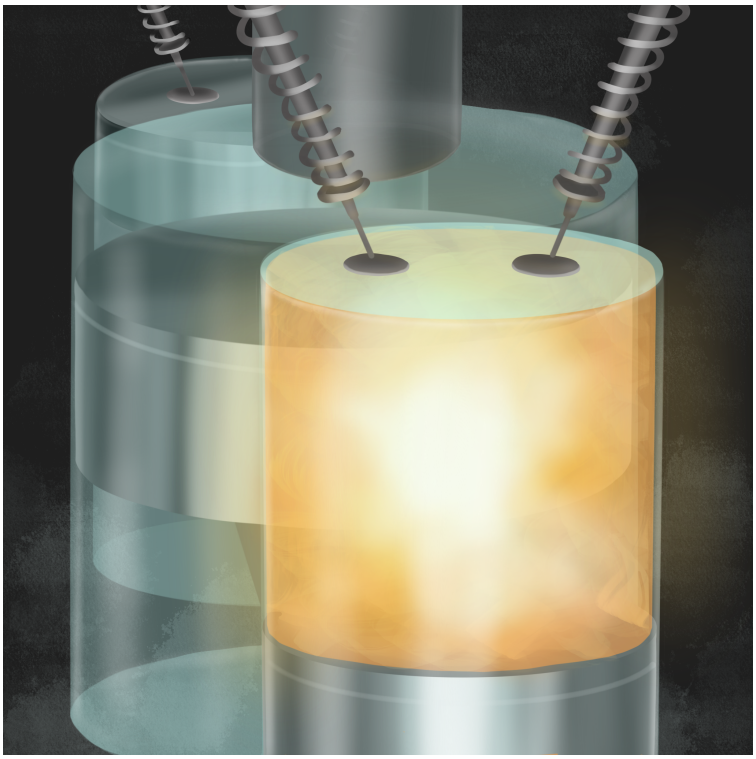

Modeling and Evaluation of the Olshammar engine

A simulation based approach of a five-stroke turbocharged engine using Siemens Amesim.

Master's thesis in Mobility Engineering

Wilhelm Hansson
Fredrik Åberg

DEPARTMENT OF MECHANICS AND MARITIME SCIENCES
CHALMERS UNIVERSITY OF TECHNOLOGY
Gothenburg, Sweden 2025
www.chalmers.se

MASTER'S THESIS 2025

Modeling and Evaluation of the Olshammar Engine

A simulation based approach of a five-stroke turbocharged engine using Siemens Amesim.

Wilhelm Hansson
Fredrik Åberg

CHALMERS
UNIVERSITY OF TECHNOLOGY

Department of Mechanics and Maritime Sciences
Division of Energy Conversion and Propulsion Systems
CHALMERS UNIVERSITY OF TECHNOLOGY
Gothenburg, Sweden 2025

Modeling and Evaluation of the Olshammar Engine
A simulation based approach of a five-stroke turbocharged engine using Siemens Amesim.
WILHELM HANSSON FREDRIK ÅBERG

Supervisor: Professor Petter Dahlander, Division of Energy Conversion and Propulsion Systems.
Inventor: Mats Olshammar, Olshammar Nebula AB.

Examiner: Professor Petter Dahlander, Division of Energy Conversion and Propulsion Systems.

Master's Thesis 2025
Department of Mechanics and Maritime Sciences
Division of Energy Conversion and Propulsion Systems
Chalmers University of Technology
SE-412 96 Gothenburg
Telephone: Wilhelm Hansson, +46 73 352 04 70. Fredrik Åberg, +46 79 348 42 48

Cover image: Olshammar Engine. Created by: Filippa Pamp

Printed by Chalmers Reproservice
Gothenburg, Sweden 2025

Modeling and Evaluation of the Olshammar Engine.
A simulation based approach of a five-stroke turbocharged engine using Siemens Amesim.
Fredrik Åberg
Wilhelm Hansson
Division of Energy Conversion and Propulsion Systems
Chalmers University of Technology

Abstract

Internal combustion engines (ICEs) have been used since the 19th century and remain relevant as of 2025, although the field faces major challenges. The future of ICEs will heavily rely on new inventions and technological advancements. This thesis addresses one such invention: the Olshammar engine, a five-stroke engine concept featuring a low-pressure exhaust cylinder. The purpose of this study is to examine how the Olshammar engine performs in comparison to a conventional four-stroke engine. There are several software tools available for modeling and simulating ICEs, and in this study, Siemens Amesim was used. Initially, a two-cylinder petrol baseline engine was modeled and optimized, providing the reference for modeling the Olshammar engine. The results show that the Olshammar engine reduces brake-specific fuel consumption (BSFC) across the operating range of 2000–5000 rpm, with the largest improvement at 3000 rpm, where BSFC is reduced by approximately 4 %. This corresponds to a fuel conversion efficiency of $\eta_f = 35.2\%$ compared to $\eta_f = 33.7\%$ for the baseline engine. Furthermore, the simulations indicate that the improvement in BSFC can be attributed to the power contribution from the exhaust cylinder, resulting from the recovery of expansion work. Additional assessment of key parameters contributing to performance improvements suggests that tuning the exhaust cylinder offset relative to the combustion cylinders, as well as adjusting the bore-to-stroke ratio, can further enhance overall performance. Siemens Amesim proved to be a well-suited tool for ICE modeling, to the extent that it could replace GT-Power in the ICE course at Chalmers in the future. Finally, the findings of this study demonstrate how the design and optimization of the Olshammar engine contribute to improved fuel efficiency compared to conventional four-stroke designs.

Keywords: Olshammar engine, Internal combustion engine, Five-stroke engine, Ilmor engine, Turbocharged engine, Low pressure cylinder, Exhaust cylinder, Siemens Amesim.

Modellering och utvärdering av Olshammar-motorn.
Ett simuleringsbaserat tillvägagångssätt för en femtakts, turboladdad motor med användning av Siemens Amesim.
Fredrik Åberg
Wilhelm Hansson
Avdelningen för energiomvandling och framdrivningssystem
Chalmers University of Technology

Abstract

Förbränningsmotorer har varit i bruk sedan 1800-talet och är fortfarande relevanta i dag, även om de möter ett ökande motstånd i samhället. Hur framtiden för förbränningsmotorer utvecklas beror i stor utsträckning på framväxten av ny teknik och nya innovativa lösningar. Detta examensarbete behandlar en sådan innovation: Olshammar-motorn, en femtaktsmotor med en lågtryckscylinder. Syftet med arbetet är att undersöka hur Olshammar-motorn presterar i jämförelse med en konventionell fyrtaktsmotor. För modellering och simulering av motorerna har programvaran Siemens Amesim använts. Inledningsvis skapades en referensmotor, en tvåcylindrig bensinmotor, som optimerades och användes som jämförelsebas mot Olshammar-motorn. Resultaten visar att Olshammar-motorn reducerar den bromsspecifika bränsleförbrukningen (BSFC) inom driftområdet 2000–5000 rpm, med den största förbättringen vid 3000 rpm, där BSFC minskar med cirka 4 %. Detta motsvarar en bränsleomvandlingseffektivitet på $\eta_f = 35,2\%$ jämfört med $\eta_f = 33,7\%$ för basmotorn. Simuleringarna påvisar vidare att förbättringen i BSFC kan kopplas till den extra effekt som utvinns ur avgascylindern som ett resultat av det extra expansionsarbetet. En ytterligare analys av de faktorer som bidrar mest till prestandaförbättring visar att finjustering av avgascylinderns förskjutning i förhållande till förbränningscylindrarna samt variation av borr- och slagförhållandet kan ge ytterligare optimeringspotential. Studien visar även att Siemens Amesim är väl lämpat för modellering av förbränningsmotorer, i sådan grad att det kan ersätta GT-Power i framtida undervisning inom ICE-kursen på Chalmers. Resultaten understryker slutligen hur designen och optimeringen av Olshammar-motorn bidrar till förbättrad bränsleeffektivitet jämfört med konventionella fyrtaktsmotorer.

Nyckelord: Olshammar-motorn, förbränningsmotor, femtaktsmotor, Ilmor-motor, turboladdad motor, lågtryckscylinder, avgascylinder, Siemens Amesim.

Acknowledgements

This thesis would not have been possible without the guidance and expertise of Professor Petter Dahlander throughout the project, so a big thank you to you, Petter. The many hours of interesting discussions with Mats Olshammar have provided great value not only to the project, but also in expanding our general understanding of new concepts related to combustion engines. We therefore greatly appreciate the support Mats Olshammar has provided. Siemens Amesim is a complex program, and without the help of Fabian Hasselby at Volupe and Gunnar Latz at Siemens, it would have been very difficult to achieve satisfying models. Lastly, thank you Christian Bosser at Chalmers for introducing us to the program and helping us get of to a smoother start.

Wilhelm Hansson and Fredrik Åberg, Gothenburg, December 2025

This page intentionally left blank.

List of Acronyms

Below is the list of acronyms that have been used throughout this thesis listed in alphabetical order:

ATDC	After Top Dead center
BDC	Bottom Dead Center
BSFC	Brake Specific Fuel Consumption [g/kWh]
BTDC	Before Top Dead center
CAD	Crank Angle Degree [°CA]
CA05	CAD where 5 % of the fuel is burned
CA50	CAD where 50 % of the fuel is burned
CA90	CAD where 90 % of the fuel is burned
EVO	Exhaust Valve Open
EVC	Exhaust Valve Close
HP	High Pressure
ICE	Internal Combustion Engine
IMEP	Indicated Mean Effective Pressure [bar]
IVO	Intake Valve Open
IVC	Intake Valve Close
LP	Low Pressure
SI	Spark ignition
TDC	Top Dead Center

This page intentionally left blank.

Nomenclature

Below is the nomenclature of variables, parameters, geometric parameters and indices that has been used throughout this thesis.

Variables

p	Pressure	[Pa or bar]
V	Volume	[m^3]
m	Mass	[kg]
$\dot{m}$	Mass flow rate	[kg/s]
u	Gas velocity	[m/s]
ρ	Gas density	[kg/m^3]
T	Temperature	[K]
h	Enthalpy	[J/kg]
E	Total energy	[J]
$W_{c,i}$	Indicated work (cylinder i)	[J]
T_{eng}	Engine torque	[Nm]
N	Engine speed	[rpm]
P	Power	[W]
$\eta_{f,b}$	Brake fuel conversion efficiency	[-]
$\dot{W}_{\text{turb}}$	Turbine work rate	[W]
Q	Heat transfer	[J]
Q_{ch}	Chemical energy of fuel	[J]
Q_{ht}	Heat transfer to walls	[J]
S	Pipe cross–sectional area	[m^2]
D	Pipe diameter	[m]
X_i	Mass fraction of species i	[-]
θ	Crank angle	[°CA]
$x_b(\theta)$	Burned mass fraction (Wiebe)	[-]
ρ	Gas density [kg/m^3]	

Parameters

R	Gas constant	[J/(kg·K)]
Q_{LHV}	Lower heating value of fuel	[J/kg]
a, m	Wiebe function parameters	[-]
θ_0	Wiebe burn start angle	[°CA]
$\Delta\theta$	Burn duration	[°CA]
C_1, C_2	Woschni heat transfer coefficients	[-]
S_w	Combustion chamber wall area	[m^2]
V_0	Cylinder volume at reference state	[m^3]
T_1, p_1, V_1	State before combustion	[K], [bar], [m^3]
f	Pipe friction factor	[-]
h_c	Convective heat transfer coefficient	[W/m^2K]
h_r	Radiative heat transfer coefficient	[W/m^2K^4]
T_{wall}	Wall temperature	[K]
PR_0	Compressor total pressure ratio	[-]
$\bar{A}$	Speed of sound ratio	[-]
ω_c	Compressor rotational speed	[rad/s]
δt	Time step size	[s]
γ	Ratio of specific heats	[-]

Geometric parameters

B	Bore	[mm]
S	Stroke	[mm]
CR	Compression ratio	[-]
L	Connecting rod length	[mm]

Indices

- i Cylinder index
- j Species index (gas composition)

This page intentionally left blank.

Contents

This page intentionally left blank.

List of Figures

This page intentionally left blank.

List of Tables

This page intentionally left blank.

1
Introduction

The objective of this chapter is to introduce the subject of the Olshammar engine. It presents the background of the concept, the research questions, the involved stakeholders and the project's main limitations. Finally, the significance of the study is discussed, followed by an outline of the report structure.

1.1 Background

Cars, motorcycles and many more transportation devices today have one thing in common, they are all typical users of a propulsion system that was invented in 1876, the four stroke ICE developed by Nicolaus A.Otto [4].

Previous to the upcoming of the four stroke ICE that is common today, Nicolaus A.Otto together with Eugen Langen introduced an atmospheric engine in 1867. That engine used the increase of pressure during combustion of the fuel and air mixture in the outward stroke to accelerate a piston. The momentum of the piston generated a vacuum in the cylinder which, combined with the atmospheric pressure, pushed the piston inward [4]. Although this engine worked, it had an modest thermal efficiency of 11 %.

Otto's introduction of the four-stroke ICE, consisting of a cycle with an intake stroke, compression stroke, expansion/power stroke and lastly an exhaust stroke, showed promising results compared to the atmospheric engine [4]. Going forward to today, the development of better performing and more efficient ICEs is still relevant. From this background, the objective of this study is to evaluate the Olshammar Engine concept, created by Mats Olshammar, by performing model based simulations in Siemens Amesim. This work is done in a collaboration with Chalmers University of Technology and Mats Olshammar at Olshammar Nebula AB.

The concept of the ICE evaluated in this project is developed by Mats Olshammar. Since 2019, Olshammar has both a Swedish and Chinese patent on the engine[15]. The idea has been developed by Olshammar and on his website [14] there are both descriptions and results of the engine. There are also 15 Youtube videos where Olshammar explains the concept in detail. With both patent and idea in place, Olshammar moved forward with the concept by doing simulations in GT- Power.

1.2 Purpose

The purpose of this thesis is divided into two parts, where the first is related to the Olshammar engine, and the second to Chalmers. For the Olshammar part, the purpose is to further analyze and evaluate the Olshammar engine, using a modeling and simulation based approach in Siemens Amesim.

For the Chalmers part of the thesis, the aim is to explore the advantages and disadvantages of Siemens Amesim in terms of ICE modeling. This is of interest for the division of Energy Conversion and Propulsion systems, and more specific the course in Internal Combustion Engines, held by Petter Dahlander. Chalmers is currently using GT-Power in the ICE course, but since the program is rather expensive compared to Siemens Amesim, it is of high interest to explore whether Siemens Amesim could be a valid replacement for GT-Power in the future.

1.3 Research questions

- How does the Olshammar engine perform compared to a four-stroke engine of same characteristics?
- How does the exhaust cylinder contribute in terms of overall performance and why?
- What is the reason for having a sideport, and what effect does it have on the engines overall performance?
- What are the advantages and disadvantages of Siemens Amesim in terms of modeling internal combustion engines?
- Should Chalmers consider the option of replacing GT-Power with Siemens Amesim in the internal combustion engine course?

1.4 Stakeholders

The stakeholders of the thesis are the following:

- Mats Olshammar: Inventor of the patent for the Olshammar engine.
- Chalmers and Petter Dahlander: It is in Chalmers interest whether the program Siemens Amesim can be implemented in the internal combustion course. Petter Dahlander is the examiner.
- Future researchers in the subject: This study can be used as a reference for future research in the field of five-stroke engines.

1.5 Limitations

- Program experience: The thesis workers experience in Siemens Amesim.
- Limited turbocharger data: Number of compressor and turbine maps in Siemens Amesim were few.
- Model simplifications: In the study, only a two cylinder gasoline engine was considered.

- Optimization: Number of parameters that could be optimized at one instance was limited by computational power.
- Knock: The available knock model in Siemens Amesim is a simplified model and only gives an indication of knock.

1.6 Significance of the study

The significance of the study is that the Olshammar concept, that in earlier studies have shown positive results regarding increased efficiency compared to conventional four-stroke ICEs, is further investigated and validated. This increased efficiency can have both positive environmental and economical effects.

1.7 Outline

The outline below presents a summary of the structure and organization in the thesis, including the main chapters and their contents.

Chapter 2 starts by exploring the field of five-stroke engines via a literature review and then proceeds by describing the Olshammar engine concept in detail. The chapter is then continued with a theoretical background that presents the fundamental parameters and theory related to the topic.

Chapter 3 presents the methods used for modeling, optimizing and validation of the Baseline and Olshammar engine. It begins by covering the basics of theory and modeling in Siemens Amesim. The chapter continues with a detailed description of the engine modeling and the optimization. Further, an analysis of the timestep and tolerance, as well as knock is presented. Lastly, the models are validated against an existing engine.

Chapter 4 presents the results of the simulations. The chapter starts with a comparison of BSFC and fuel conversion efficiency. It proceeds by examining the contribution of the sideport and the effect of different exhaust cylinder geometries, as well as the timing in CAD of the exhaust cylinder related to the combustion cylinders. The chapter ends by presenting the difference in flow properties for different sections of the Baseline and Olshammar engine.

Chapter 5 begins by analyzing the results of Chapter 4, with respect to how the exhaust cylinder contributes. It follows by discussing the complications that occurred when attempting to model the Ilmor engine and then dives into the sensitivity analysis that highlights the connection between parameters and robustness of the models. The modeling of ICEs in Siemens Amesim is further discussed, with reasoning of the advantages and disadvantages compared to GT-Power. The chapter ends by addressing the results of this study in comparison to previous work on the Olshammar engine.

The thesis is concluded in Chapter 6, that showcase the potential of the Olshammar engine and how Siemens Amesim can be used for modeling ICEs in the ICE course at Chalmers.

This page intentionally left blank.

2

Literature Review and Theoretical Background

This chapter provides the theoretical foundation for the study and is divided into two main parts. The first part presents a literature review of modern engines and previous work on five-stroke engine concepts, while the second introduces fundamental ICE theory. Together, these sections establish the background knowledge required for the modeling work described in Chapter 3.

2.1 Literature review

The concept of five-stroke engines is not new, several attempts have been made to develop efficient engine configurations based on this principle. This section reviews some of the most notable five-stroke concepts and their main characteristics. In addition, previous work related to the Olshammar engine is presented.

2.1.1 State of the art technology and engines today

In recent years, the automotive industry has seen many different engine concepts that show greater performance and efficiency than before, and the development of new technology progress fast. Heywood stated in 2018 that the best BSFC of a four-stroke turbocharged gasoline engine at that time was 230 g/kWh [4], but in recent years, this value continues to decrease, meaning even more efficient engines. A modern state of the art engine is the Mercedes-AMG 2.0-liter M139 engine, a turbocharged four-cylinder engine that produces 416 hp [22]. The engine has a two-stage fuel injection, as well as a spray guided combustion process that helps to increase thermodynamic efficiency. In addition, the compression ratio is 9 and the max boost pressure is 2.1 bar (absolute pressure 3.1 bar) for the S-model. There is no official data published related to brake specific fuel consumption or overall efficiency of the engine.

2.1.2 Previous results of five-stroke engines

There has been many previous studies related to the topic of five-stroke engines with turbochargers for the purpose of achieving increased power and efficiency. In 2003 the Belgian engineer Gerhard Schmitz filed a patent of a five-stroke ICE that showed increased power density compared to a regular ICE[3]. The engine consists of two HP combustion cylinders and one LP exhaust cylinder, with larger swept volume than the HP combustion

cylinders[8]. In this concept, instead of directly transferring exhaust gases into the atmosphere, the exhaust gases are sent to the LP exhaust cylinder to achieve an extra expansion stroke with high expansion ratio [17].

High power density of engines is usually desired to reduce weight and dimensions[3]. Increase of power density can be achieved by increasing the air-intake by using compressed air. Schmitz stated that the advantages in terms of power for an controlled ignition engine using gasoline resulted in an increase in energy output of 20% at full load and 25% at partial load. For the case of a compression ignition engine using Diesel, the increase in energy output was in the range of 14% to 25%.

Another study on a five-stroke engine with port fuel injection and spark ignition was performed in 2014 [8]. One of the key aspects of this study was to look into how a five-stroke engine could be used as a range extender, whereas it would mainly operate in high efficiency operating points. The ICE in this study utilize a "smart wastegate" system with variable valve timing to control the boost pressure of the turbocharger. The study performed tests over a wide range of operating points, however, the results were mainly presented for an engine speed of 4000 rpm and brake power of 32.8 kW. At this operating point, the BSFC was 226.4 g/kWh, which corresponded to an efficiency of 36.1% for the engine [8]. Compared to an engine with the same displacement using the Miller cycle, the five-stroke ICE showed greater power density. It was mentioned that the knock factor was one limitation of the performance, and that fuel with higher octane number could be further investigated to overcome this limitation.

Downsized engines are highly relevant today, and in 2016, Li, T. et al., performed a study to showcase whether a Miller cycle or a five stroke cycles was beneficial for downsized, highly boosted SI engines [9]. Different configurations of the Miller cycle was studied, such as EIVC140, LIVC60 for low load operation, and LIVC80 for high load operation. The first comparison of low load operation included a Miller cycle with EIVC140 and one with LIVC60. In the studied case, the Miller engine's fuel conversion efficiency was better than the five stroke engine, but both the Miller and the five-stroke where in turn better than the Otto cycle engine in terms of fuel conversion efficiency [9]. Li, T. et al.(2016) relates this to lower pump losses compared to the original engine, 2.8% lower for EIVC140 and 4.5% lower for LIVC60. The five-stroke engine however experienced higher pumping losses compared to the original engine. For the high load operation case, the five-stroke engine achieved a higher fuel conversion efficiency than both the Miller cycle and original engine. This was by the authors claimed as a result of the five-strokes "cooling effect of the inner expansion cylinder on elimination of fuel enriched operation" [9].

Stuart, K. et al.(2017) conducted a thermodynamic analysis of the five-stroke engine in 2017 where the thermal efficiency and power output over a wide range of operating points were analyzed [20]. Stuart, K. et al. states that there has been mixed results in previous studies regarding the efficiency of a five-stroke engine. Where some results state an efficiency of 36% and others 30%, and that few of these studies have included in- cylinder heat transfer and mass losses due to blow-by. The Wiebe function is used for the heat

release analysis, as well as a 0D engine model that includes heat transfer via the cylinder walls and mass loss due to blow-by. The results of the study showed that the five-stroke engine achieved an indicated efficiency of 32%, which was an increase of 6% compared to the Otto cycle engine that also was used in the study. overall, the five-stroke engine showed up to 10% increased efficiency over a wide range of operating parameters. In terms of heat transfer analysis, Stuart, K. et al. conclude that the 5th stroke contribute with a large heat loss of up to 41% of the entire cycle's total loss.

There has also been several physical implementations of five-stroke ICEs, mainly based on modified four-stroke engines. Such an engine was built at Cracow University of Technology by Noga.m [12]. The engine used in this study is a four-cylinder turbocharged SI engine from Audi, with a power of 147 kW and a displacement volume of 1.984 dm^4[12]. A series of test results of the original engine was performed to get reference results for the five-stroke engine. The main re-design went into designing the cylinder head and camshafts, as well as manifolds and the boost system. During testing, the modified five-stroke IC engine showed decreased BSFC in middle range RPM, as well as increased specific power for the entire speed range compared to the four-stroke ICE.

2.1.3 The Olshammar engine concept

The purpose of the Olshammar engine is to further improve turbocharged ICEs efficiency and performance [15]. To get to the core of how this is achieved, one has to understand that the exhaust gases generated from the combustion process in the combustion-cylinders, contains a significant amount of energy that can be converted to work by the turbocharger[15]. A turbochargers efficiency is highly dependent on the mass flow entering the turbine, whereas it is advantageous if low mass flow comes in pulses, and large mass flow in a more constant flow[15].

A configuration of the Olshammar engine, consisting of one exhaust cylinder(1) with a sideport(23), a pipe without valve connecting the exhaust cylinder and turbine inlet(17), two combustion cylinders(2,3), and a turbocharger arrangement (26,27) is shown in Figure 2.1.

In the low pressure (LP) exhaust cylinder, there are no intake or exhaust valves, which differs from the concept of the original five-stoke engine by Gerhard Schmitz [3] that has exhaust valves on the exhaust cylinder. This difference allows for a more constant flow to the turbine in the Olshammar engine [14]. More even flow could potentially increase turbine efficiency, and as a result the performance of the engine [15]. Additional performance gain comes from the exhaust cylinder that extracts work from the pressure pulses and therefore increases the output torque on the crankshaft. This further result in higher efficiency. In addition, the added exhaust cylinder also helps with limiting back-pressure of the combustion cylinders. Since the exhaust cylinder expands while the exhaust valve of the combustion cylinders is open, the exhaust gas is split between the exhaust cylinder and the exhaust duct, allowing the exhaust gas to evenly distribute between the exhaust duct and the exhaust cylinder [15].

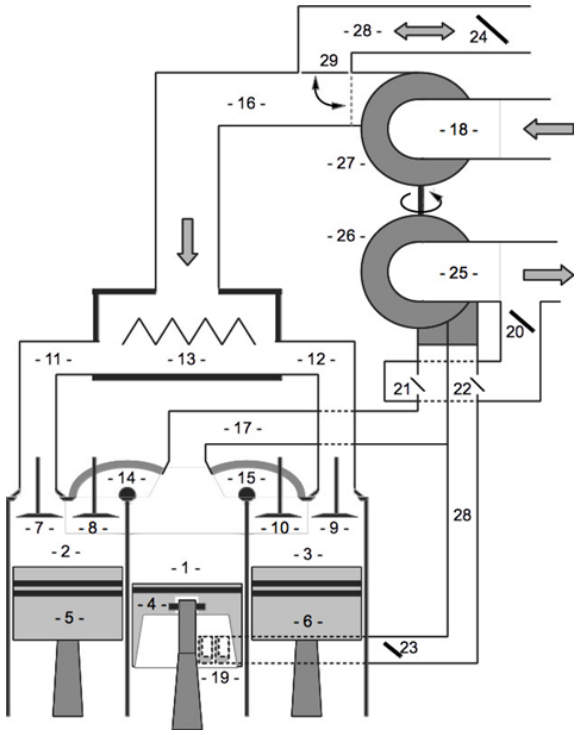

Figure 2.1: The Olshammar engine. 2+1 cylinder configuration with sideport.

2.1.4 Master's Thesis at KTH in 2021

After Olshammar developed the concept of the engine, it was further investigated in a masters thesis in 2021 at the royal institute of technology (KTH) in Sweden. The master thesis had several similarities to this project. It evaluated and simulated the Olshammar engine using the software GT-Power which, just as Siemens Amesim, is a program that can model ICEs. In GT-Power, a four-cylinder SI engine was imported and modified to a baseline 2 cylinder SI engine. The baseline was then modified to the Olshammar engine with configuration 2+1 (two combustion cylinders and one exhaust cylinder) [10]. The two configurations were then compared and evaluated on BSFC, BP, turbocharger efficiency, impact on muffler and after treatment system sizing, hardware modification and flywheel inertia. The project concluded that performance of the Olshammar engine increased with boost pressure. With an absolute boost pressure of 3.5 bar, an average reduction in BSFC with 5% and an increase of 4% in brake power were seen compared to the baseline model for the range from 2000 to 6500 rpm.

At 3.5 bar absolute boost pressure and 4500 rpm the peak torque of the baseline and the Olshammar engine were compared. Since the brake torque was different for the models, a normalized brake torque was used and calculated "by dividing the instantaneous torque by the average torque value at that operating engine speed" [10]. For the Olshammar engine, the normalized brake torque were 6% smaller which lead to the conclusion that a smaller and more compact flywheel could be used. It is worth taken into account that the normalized brake torque comparison were done at the best operating point for the Olshammar compared to the baseline model.

The thesis at KTH[10] states that the turbocharger efficiency is improved as a result of the observed smoother exhaust gas flow to the turbine for the Olshammar model. However, there is no measurements taken from the turbocharger that supports this.

The project ends with a recommendation for future work where "diesel engines for heavy-duty applications and large-bore four-stroke marine engines" is encouraged to be more investigated in combination with the Olshammar engine [10]. A future developer is also encouraged to asses the Olshammar concept for an existing engine with compressor and turbine maps available. Lastly, the thesis mentions that using a semi predictive combustion model could have some benefits.

2.1.5 FEV Engineering Simulations

To further understand the potential of the Olshammar engine, Olshammar contacted the consulting company FEV Sverige AB and performed new simulations in GT-Power in October 2023. Olshammar refers to the results as very good on his website [14], they can be seen in Table 2.1.

Engine Type	BSFC Decrease (%)	BP Increase (%)	Boost Pressure (bar)
Four-stroke Petrol (SI)	10.1	16.4	3.5
Four-stroke Diesel (CI)	8.2	19.2	5.5
Two-stroke Diesel (CI)	24.8	95.8	5.5

Table 2.1: Performance improvement for Olshammar engine compared to Baseline engine

In the report where FEV engineering concluded the results, several different engine configurations were tested [21]. In Table 2.2 and 2.3, the comparison of a baseline and Olshammar two cylinder petrol engine with one liter in total cylinder displacement is shown. In the Δ columns, the relative change in % shows that the Olshammar model performs better for all rpm, both when it comes to BSFC and BP (exception BP at 5000 rpm for 3.5 bar boost).

RPM	Absolute Boost [bar]	BSFC Baseline [g/kWh]	BSFC Olshammar [g/kWh]	ΔBSFC [%]	BP Baseline [kW]	BP Olshammar [kW]	ΔBP [%]
2000	3.5	212.86	205.76	-3.34	44.73	72.79	+62.74
3000	3.5	207.98	188.32	-9.45	102.14	120.44	+17.92
4000	3.5	211.07	190.66	-9.67	153.12	177.59	+15.98
5000	3.5	218.87	199.99	-8.63	183.74	181.19	-1.39

Table 2.2: Comparison between Baseline and Olshammar engine at 3.5 bar boost

Looking at the results from FEV raises a few questions. Firstly, there is no reasoning about the results, they are simply published in a PowerPoint [21]. The low BSFC is also questionable when compared to modern real world, state of the art, engines. The simulations also showed that the petrol engine could achieve lower BSFC than the diesel engine, which seems unreasonable in comparison to existing engines on the market. Further, the

RPM	Boost [bar]	BSFC Baseline [g/kWh]	BSFC Olshammar [g/kWh]	ΔBSFC [%]	BP Baseline [kW]	BP Olshammar [kW]	ΔBP [%]
4000	2.5	214.89	199.24	-7.28	109.02	122.60	+12.46
4000	3.0	212.70	193.94	-8.82	131.19	150.43	+14.67
4000	3.5	211.07	190.66	-9.67	153.12	177.59	+15.98
4000	4.0	209.74	188.50	-10.12	174.43	204.21	+17.07

Table 2.3: Comparison between Baseline and Olshammar engine at 4000 rpm for different boost pressures

choice of comparing the Olshammar engine to the Baseline engine at specifically 4000 rpm for the boost variations is not clearly motivated, and it is not an usual operating point to compare engines at. A more suitable range for the operating point would be 1500-2000 rpm.

2.2 Theoretical Background

To provide an overview of the fundamentals of ICEs, this section presents the key performance parameters and theoretical concepts relevant to the study including knock, turbocharging and the four stroke cycle.

2.2.1 Indicated work

Following the pressure trace from a pressure- volume diagram seen in Figure 2.2, the work transfer from the gas mixture to the piston over a cycle can be obtained [4].

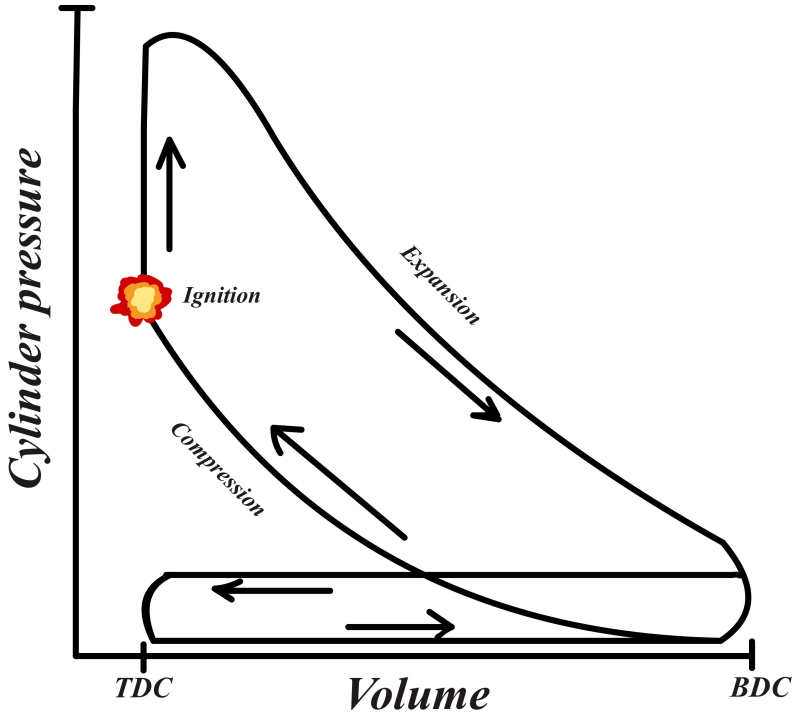

Figure 2.2: P-V diagram of a four-stroke engine.

By integrating the pressure over the volume for the entire cycle, the indicated work is defined by Equation (2.1).

$$W_{c,i} = \int p dV \tag{2.1}$$

2.2.2 Brake power and brake torque

In an ICE context, torque is used as a measure of how much work the engine produces. It can also, together with the angular velocity, be used to calculate the rate at which work is produced. This corresponds to the output power, see Equation (2.2) where P is the power [W], N is the rotational speed [rev/s], and T is the torque [Nm] [4].

$$P = 2\pi NT \tag{2.2}$$

The power and torque can be measured at the crankshaft. This is done for a specific load or brake meaning that brake torque and brake power is the effective output. These are parameters that are frequently used when evaluating engine performance [4].

2.2.3 Brake Specific Fuel Consumption

Brake specific fuel consumption, hereby mentioned as BSFC [g/kWh], is a parameter that describes how much work an engine can produce given a certain amount of fuel, defined by Equation (2.3)[4]. The parameter BSFC is normalized which makes it independent of the engine size. According to Heywood the SI-engines with the lowest BSFC have typical values around 235 g/kWh [4].

$$BSFC = \frac{\dot{m}}{P_b}, \tag{2.3}$$

where $\dot{m}$ is the mass flow rate [m/s] and P_b is the brake power [W].

2.2.4 Brake Fuel Conversion Efficiency

Brake fuel conversion efficiency is defined as the ratio of power output to chemical energy input [4]. The formula in terms of BSFC is defined as

$$\eta_{f,b} = \frac{3600}{BSFC\ Q_{LHV}}, \tag{2.4}$$

where Q_{LHV} is the lower heating value of the fuel, and defines the energy content. Standard values of Q_{LHV} for hydrocarbon fuels are in the range of 42-44 MJ/kg [4].

2.2.5 Four-stroke Cycle

A four-stroke cycle is defined by an entire cycle being completed in four strokes, or 2 crankshaft revolutions for each expansion stroke[4]. The cycle starts with the intake stroke where the piston moves from Top Dead Center (TDC) to Bottom Dead Center (BDC), in order to pull fresh air into the cylinder. In general, the intake valve opens prior to TDC to further increase volumetric efficiency. The intake valve closes shortly after the intake stroke ends for the same reason. When the intake stroke is completed, the piston is at position BDC and the compression stroke starts. During the compression stroke, the piston compresses the air fuel mixture. When the piston reach TDC, combustion starts either by compression (CI-engine) or a spark (SI-engine) which results in a instantaneous rise in pressure in the cylinder. After combustion is initiated, the expansion stroke starts

at TDC and ends at BDC. During this stroke, the gases in the cylinder have high pressure and temperature, which pushes the piston down towards BDC, resulting in a force on the piston which make the crankshaft rotate. The last stroke, the exhaust stroke starts from BDC and ends at TDC, pushing the burned gases out from the cylinder to the exhaust [5].

2.2.6 Five stroke Cycle

The concept of the five stroke cycle was developed by the Belgian engineer Gerhard Schmitz [3]. The concept is based on a configuration of at least one high-pressure (HP) combustion cylinder connected to at least one low-pressure (LP) exhaust cylinder. The HP combustion cylinder adapts a four stroke cycle, and the LP exhaust cylinder adapts a two stroke cycle, by first expanding the exhaust gases entering from the HP combustion cylinder, and then pushing these gases out of the cylinder with a fifth expansion stroke[3]. This expansion stroke can utilize an expansion ratio that is of a larger magnitude than the compression ratio in the HP combustion cylinders[17].

2.2.7 Knock

In a combustion engine, abnormal combustion can occur when the unburned fuel–air mixture ahead of the propagating flame front (the end gas) auto-ignites due to high pressure and temperature. This rapid and uncontrolled release of chemical energy generates pressure waves that resonate within the combustion chamber. This phenomenon is known as knock, which can cause severe engine damage [4]. Knock may arise for different reasons, such as overly advanced spark timing or surface ignition from local hot spots that ignite the mixture before the flame front arrives.

2.2.8 Miller cycle

For a four-stroke engine, the gas pressure inside the cylinder is greater than the pressure in the exhaust system when opening the exhaust valve. Therefore, energy contained in the high pressure cylinder gases are wasted in the exhaust system [4]. A solution to this, where more of the available energy is used, is the Miller cycle. According to [7], using the Miller cycle can improve the thermal efficiency compared to a conventional four-stroke engine. This can either be achieved with a late or early intake valve closing which reduces the compression stroke without affecting the combustion. However, while the thermal efficiency is increased, the reduced compression stroke means less air in the cylinder which reduces the BMEP [7]. To account for this, a Miller cycle engine is combined with a turbocharger or a supercharger that increase the pressure of the intake air which compensates for the shorter compression stroke. In this way, the BMEP can remain on high levels while the thermal efficiency is improved. Lastly, the improved thermal efficiency and the cooling effect from the intake air caused by the intake valve timing, helps to reduce the risk of knock due to pre-ignition in an SI-engine [7].

2.2.9 Turbocharging Principles

A turbocharger consist of a compressor linked mechanically via a shaft to a turbine. The main purpose of a turbocharger is to increase the overall power density of the engine. It is a heavily used concept and is typically used in order to be able to downsize engines. By directing the exhaust gases from the cylinder to the turbine after the exhaust stroke, the remaining energy in the exhaust gas spins the turbine, and since it is connected via a shaft to the compressor, the compressor starts to rotate and compress air that is led to the intake of the cylinder. Maximum power in an engine is limited by airflow entering the cylinder each cycle. By compressing the air prior to entering intake of the cylinder, the density of the air is increased and thereby the power output of the engine rises [6].

By assuming that the turbocharger can be placed in a defined control volume, Equation (2.5) show that the power is related to the energy of the gas/mixture[4].

$$\dot{Q} - \dot{W} = \dot{m}\left[\left(h + \frac{C^2}{2} + gz\right)_{out} - \left(h + \frac{C^2}{2} + gz\right)_{in}\right]. \tag{2.5}$$

The heat transfer rate $\dot{Q}$ is typically a low value and can therefore be removed, resulting in the expression below.

$$-\dot{W} = \dot{m}(h_{0,out} - h_{0,in}) \tag{2.6}$$

This expression represents the rate of shaft-work transfer (power) leaving the control volume, where $\dot{m}$ is the mass-flow rate and h_0 denotes the stagnation enthalpy.

A turbocharger works efficiently when the incoming flow is steady, which is not usually the case if the flow directly comes from the cylinder where the flow is pulsating [4]. To overcome unsteady flow to the turbine, an exhaust manifold of large volume is used to even out the pressure pulses from the exhaust runner. This helps to achieve close to steady flow, but with the drawback that energy losses occur in the process of dampening the high energy pressure waves[4].

To further increase volumetric efficiency, an intercooler can be used to decrease the air temperature and thereby increase its density [4]. The intercooler is located after the compressor and before the intake manifold [6].

To control the amount of boost pressure in the intake, a wastegate is used to allow exhaust gas to bypass the turbine [6]. The wastegate is placed upstream in the exhaust manifold or more common today, directly in the housing of the turbine [6]. Moreover, the wastegate contributes to limiting knock in the engine, as well as ensuring that there is obedience with the limits of both the compressor and turbine maps [6].

This page intentionally left blank.

3
Methodology

The objective of this chapter is to describe the engine modeling process. After becoming familiar with the software, the Olshammar model was constructed, optimized and evaluated in comparison to a baseline configuration.

3.1 Siemens Amesim

The software used for modeling and simulating the Baseline and Olshammar engine was Siemens Amesim version 2410. Siemens describes the software as follows on their about page for the program [18], "Simcenter Amesim is a mechatronic systems simulation platform that allows design engineers to virtually assess and optimize the systems' performance". With no prior experience using Amesim, a hands on study of the program started the project. Since GT-Power was, and had been for several years, the main program of use for simulating combustion engines at Chalmers, there was not a lot of easy access guidance in the program. Siemens own tutorials, demos and library documentation were therefore the main source of learning material during the early stages of the project.

There are different libraries in Amesim that are used to construct and build models. In the case of this project, the mainly used libraries are the IFP-Engine library and the CFD1D library. By using these two libraries, it is possible to construct the different engine configurations in this project, the Baseline model and the Olshammar engine model. Generally when designing engine models in Amesim, it's well sufficient and in most cases good enough to only use the IFP-Engine library, but in the scope of this project that relies heavily on accurate gas- modeling in the intake and exhaust, the CFD1D library is used for that purpose.

3.2 Modeling theory

This section describes the modeling approaches used in Amesim for the main processes of the combustion engine including combustion modeling, knock prediction, thermodynamic modeling in 0D, gas modeling in 1D and the turbocharger behavior.

3.2.1 Thermodynamic Modeling in 0D

The cylinder volume is typically modeled as a thermodynamic system using the conservation equations for mass and energy [4]. This approach assumes that the gas properties

within the cylinder are considered uniform at each point in time, that is the system is treated as a zero-dimensional control volume. In the cylinder volume region, the total rate of change of mass flow equals the difference between flow in and out of the region, shown below in equation (3.1)

$$\dot{m} = \sum \dot{m}_j. \tag{3.1}$$

The energy transfer in the region is described by equation (3.2)

$$\delta Q_{ch} = \delta U_s + \delta Q_{ht} - + \delta W + \sum_j dm_j h_j, \tag{3.2}$$

where δQ_{ch} is the chemical energy of the fuel, δU is the internal energy, δQ_{ht} is the heat transfer, δW is the change of work and $dm_j h_j$ is the enthalpy over the boundaries.

For an ICE, the heat transfer play a crucial role when it comes to both design, efficiency, emissions and performance. With temperatures of the burning gasses reaching as high as 2500 Kelvin, heat transfer appears between the gas inside the cylinder and the cylinder walls, lining and head [4]. The magnitude of heat transfer affects several parameters. For example the need of a cooling system to protect engine parts, efficiency and the formation of different emissions. According to Heywood (2019), an increase of heat transfer to the chamber walls will lower gas temperature and pressure [4]. This results in reduced piston work which reduces the efficiency and power output from the engine.

The heat exchange between the fluid in the cylinder and the cylinder walls (Q) are computed using the Woschni equation, see Equation (3.3). Descriptions and units of each variable is found in Table 3.1 from the Amesim documentation [2].

$$Q = \frac{130 \cdot p^{0.8}}{T^{0.53} \cdot \text{Bore}^{0.2}} \cdot \left(C_1 \cdot V_p + C_2 \cdot \frac{V_0 \cdot T_1}{p_1 \cdot V_1} \cdot (p - p_0) \right)^{0.8} \cdot \text{Sw} \tag{3.3}$$

Symbol	Description	Unit
V_p	Mean velocity of the piston	m/s
stroke	Engine stroke	m
ω	Engine rotational speed	rad/s
p	Pressure in the combustion chamber	bar
T	Temperature in the combustion chamber	K
C_1, C_2	Woschni model coefficients (cycle phase dependent)	–
V_0	Combustion chamber volume	m^3
P_1, T_1, V_1	Pressure, temperature, and volume before combustion	bar, K, m^3
P_0	Pressure without combustion	bar
S_w	Surface area of the combustion chamber wall	m^2

Table 3.1: Description and units of engine simulation variables

3.2.2 Combustion modeling

To simulate the combustion process in the cylinder, the built in Wiebe function was used in Amesim. The function can be seen in Equation (3.4) and describes the mass fraction burned versus crank angle degrees [4]. The shape of the Wiebe function can be changed using the parameters a and m (standard values are a=5 and m=2). Rogers and Martyr (2021) also describes the Wiebe function as widely adopted for modeling the heat release in a combustion process by creating a similar burn curve as the S-shape of the heat release integral. In conclusion, by using the Wiebe function a representation of how the air fuel mixture burns in a real engine can be achieved for the model in Amesim [11].

$$x_b(\theta) = 1 - \exp\left[-a\left(\frac{\theta - \theta_0}{\Delta\theta}\right)^{m+1}\right] \tag{3.4}$$

With the Wiebe model working for the engine, it had to be tuned in order to achieve high performance and realistic values. According to Pulkrabek and Willard (2004), the burn duration for most engines is around 25 CAD [16]. Pulkrabek et al. also mentions that a typical spark ignition is around 10-30 CAD BTDC, this is a general value and apply for different engines. Lastly CA50 was studied to validate the models. To reduce emissions and increase the performance and efficiency of the engine, a CA50 around 8-12 CAD ATDC has in earlier studies shown best results [13]. This value is also supported by Heywood (2019) stating that for MBT timing in the general engine, CA50 will occur around 5-7 CAD ATDC [4]. By using the mentioned values (burn duration, CA50, spark ignition) for the combustion and confirming they stayed withing a valid range when optimizing, the model could be optimized while maintaining a high trustworthiness.

3.2.3 Knock modeling

When modeling an ICE, including knock analysis can increase the validity of the model. Knock serves as the upper limit for performance by limiting how high compression ratio, boost pressure and efficiency the model can have. The knock model that Amesim provides interpolates the ignition delay time from precomputed tables. These values are then used in the Livengood–Wu integral to predict the timing of auto-ignition, where knock is assumed to occur when the integral reaches unity [2].

The output of the knock model is provided as the parameter “BMF when knock detected” where BMF stands for burned mass fraction. To classify an event as knock, a threshold for the BMF is defined. In this project, the threshold is set to 0.85 for all models, meaning that if auto-ignition occurs before 85% of the fuel mass fraction is burned, the event is categorized as knock. It should be noted that this value is an approximation. Despite efforts during the literature review, no suitable reference specifying at what BMF level knock typically occurs in the end gases could be found. Since 0.9 is used as the default threshold in Amesim, a value of 0.85 was selected to include a safety margin relative to the default setting.

3.2.4 Gas Modeling In 1D

An important aspect in terms of modeling combustion in an engine is the fact that gases are usually treated as ideal gases [4]. The ideal gas law, shown in Equation (3.5), states the relation, for a given mass m, between the pressure p, volume V, gas constant R and temperature T.

$$pV = mRT \tag{3.5}$$

The intake and exhaust manifolds as well as the turbocharger are modeled using a one dimensional approach with the CFD1D library. This is achieved by discretization of each part into N-1 cells with size δx and solving the governing equations for continuity, momentum and energy at each cell center at each timestep δt [1]. The governing equations are shown by Equation (3.6), (3.7) and (3.8).

Continuity equation:

$$\frac{\partial \rho_i S}{\partial t} + \frac{\partial \rho_i u S}{\partial x} = 0. \tag{3.6}$$

Momentum equation:

$$\frac{\partial \rho u S}{\partial t} + \frac{\partial (\rho u^2 + p) S}{\partial x} - p\frac{\partial S}{\partial x} + \frac{1}{4} f \|u\| \rho u \sqrt{\pi S} = 0. \tag{3.7}$$

The total energy equation

$$\frac{\partial \rho E S}{\partial t} + \frac{\partial (\rho E + p) u S}{\partial x} - 2\left(h_c(T_{\text{wall}} - T) + h_r(T_{\text{wall}}^4 - T^4)\right)\sqrt{\pi S} = 0. \tag{3.8}$$

Defining a gas in a pipe is achieved by considering its density ρ, static pressure p and stream velocity u. Since the gas in this case is simulated using both the IFP-Engine library and the CFD1D library, a mass fraction term X, also has to be considered:

$$\sum_i X_i = 1. \tag{3.9}$$

The temperature T is defined as a function: $T(\rho, p, X)$.

Each parts (pipes) section is defined as S:

$$S = \pi \left(\frac{D}{2}\right)^2 \tag{3.10}$$

Another important aspect is the heat transfer for the energy contained in the exhaust gasses. Less heat transfer leads to hotter exhaust gases which can increase the efficiency of exhaust energy driven devices such as turbochargers and emission after treatment systems [4].

3.2.5 Turbocharger Modeling

Modeling a turbocharger in 1D is achieved by connecting a turbine to a compressor from the CFD1D library with an inertia from the Mechanical library as a link, seen Figure 3.1.

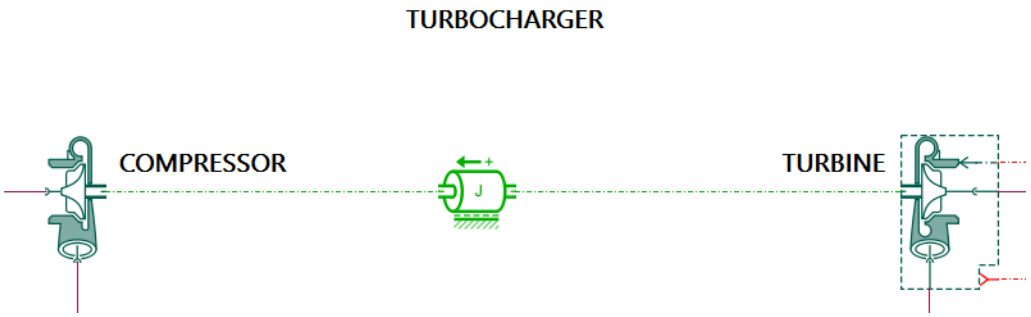

Figure 3.1: Turbocharger 1D

The compressor and turbine models use a Riemann solver in combination with a so-called performance map to simulate the thermodynamic behavior of the working gas [1].

Compressor

The governing equations used as input to the Riemann solver for the compressor are given below [1].

Continuity equation

$$\rho_1 u_1 S_1 = \rho_2 u_2 S_2, \tag{3.11}$$

Total pressure ratio

$$PR_0 = \frac{P_{0,2}}{P_{0,1}} = map(\dot{m}_c, \omega_c), \tag{3.12}$$

Speed of sound ratio

$$\bar{A} = \sqrt{\frac{T_{0,2}}{T_{0,1}}} = map(\dot{m}_c, \omega_c). \tag{3.13}$$

Turbine

The equations used as input to the Riemann solver for the turbine are formulated in a similar way to those for the compressor [1].

Continuity equation

$$\rho_1 u_1 S_1 = \rho_2 u_2 S_2, \tag{3.14}$$

Corrected mass flow rate

$$\dot{m}_c = map(PR_0(\omega_c)), \tag{3.15}$$

Efficiency

$$\eta = map(PR_0, \omega_c). \tag{3.16}$$

An example of the compressor and turbine performance maps is shown in Figure 3.2. These maps are highly useful for evaluating the performance of the turbocharger and assessing the validity of simulation results, as discussed further in the sensitivity analysis 5.2.

The compressor map consists of four boundary regions [1]:

- Low-speed extrapolation
- Maximum-speed extrapolation
- Surge extrapolation
- Choke extrapolation

Where the low and max speed boundary indicate that the compressor operate outside of the lower and upper limit of the defined map due to either to low or to high speed. In surge, the compressor operate to the left side of the present map which indicates low values of corrected mass flow rate, and finally there is choke which indicates high values of corrected mass flow rate, limited to sonic choke[1]. The efficiency map of the compressor can be scaled in Amesim, which turned out to give high flexibility in the models.

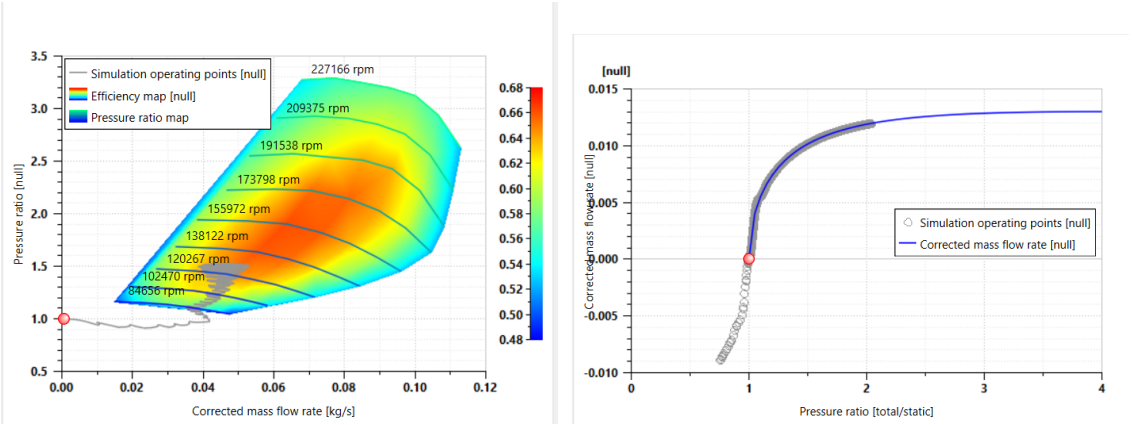

(a) Compressor Map **(b)** Turbine Map

Figure 3.2: Compressor and turbine map.

3.3 Engine Modeling

With all the necessary components and submodels in place, the two models could be modeled in Amesim. The models are presented in the sections below and consists of the Baseline and Olshammar model.

3.3.1 Baseline

The first engine modeled was the Baseline, it was from this model that the Olshammar engine later was developed. After familiarizing with the program and studying demo models available in Amesim, a four cylinder SI engine with a displacement volume of 2 liters was chosen as a foundation to build the Baseline upon. It can be seen in Figure 3.3 and includes controllers for exhaust particles, fuel injection, the throttle and the wastegate. Since the demo file used the IFP-engine library for intake and exhaust system, it had to be replaced with components from the CFD1D library in order to model the gas flow in more detail. Both the controller for the throttle and exhaust particles were removed as these fell outside the scope of the project. In practice, this meant that the cylinders, fuel system and the wastegate controller were kept while the remaining parts were replaced when moving from the demo to the Baseline model.

After changing the intake/exhaust system, the turbocharger and making modifications in submodels and parameters, the model in Figure 3.4 was achieved.

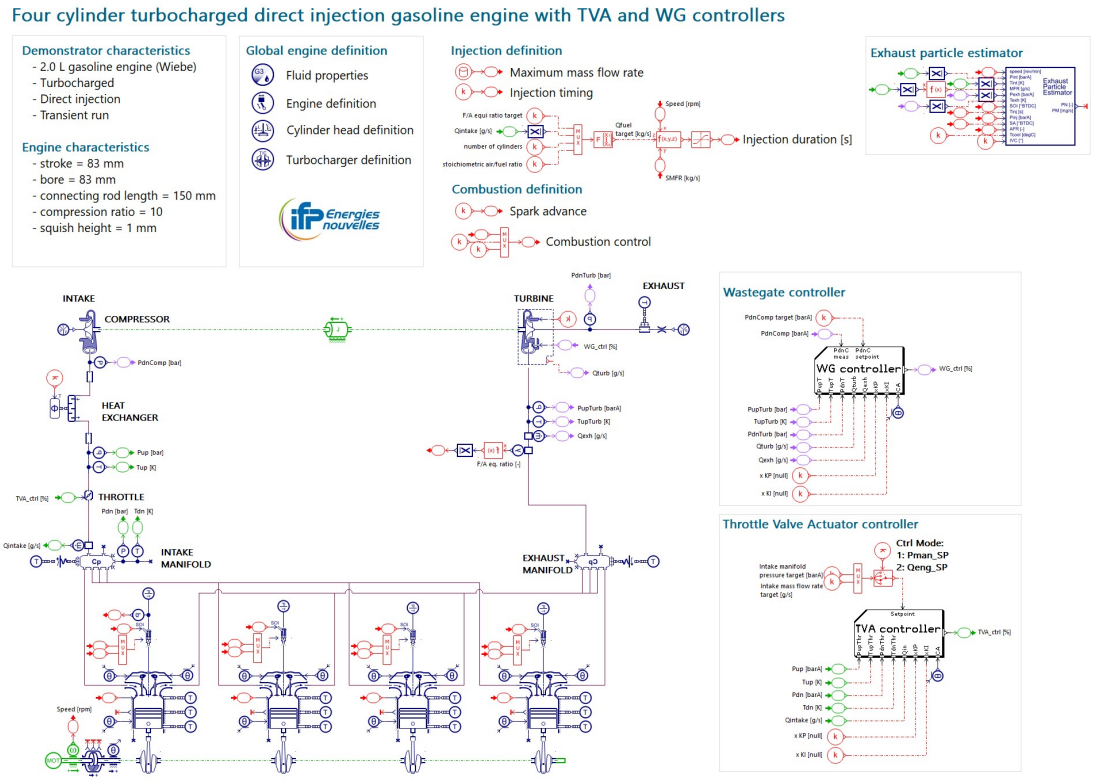

Figure 3.3: Demo model

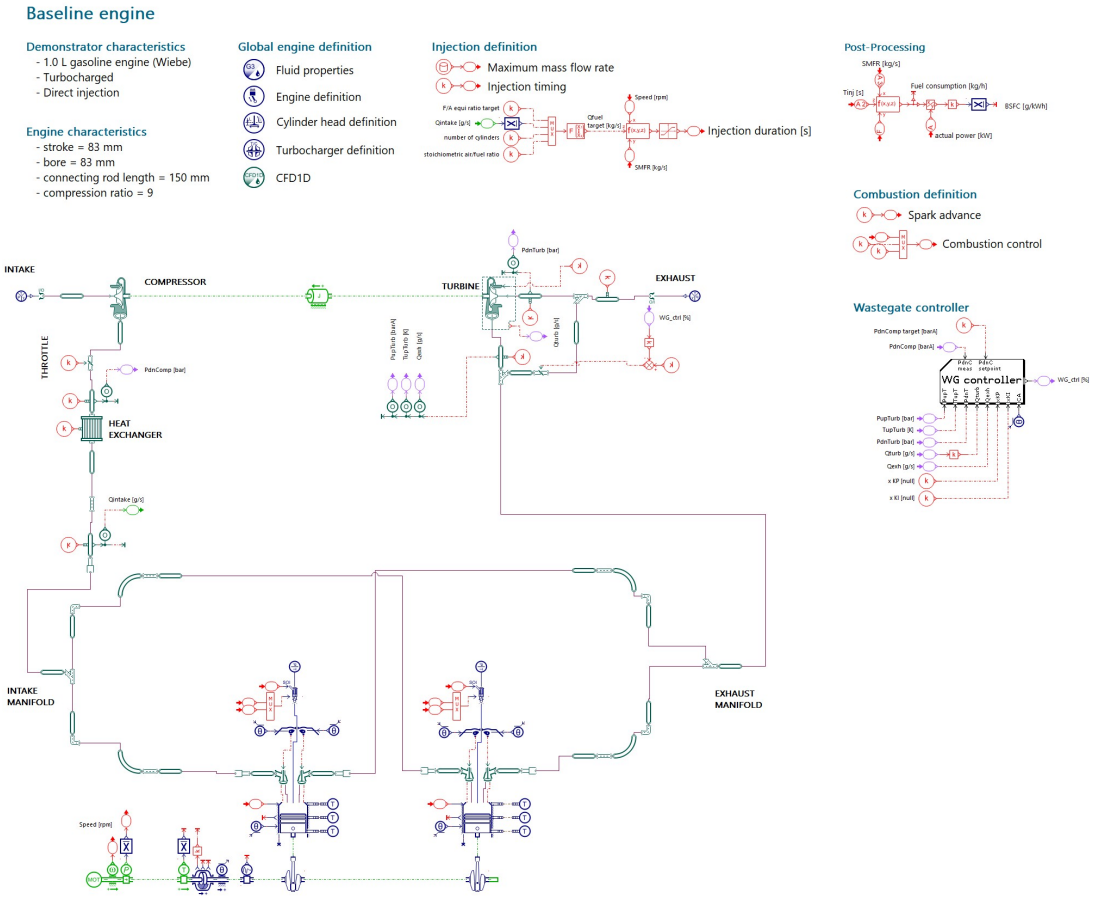

Figure 3.4: Baseline model

Intake and exhaust

As earlier mentioned, the intake and exhaust system were modeled using components from the CFD1D library (green components in Figure 3.4). Atmospheric pressure and temperature were applied as the initial conditions throughout the entire intake and exhaust system, as well as constants in the pressure source at the inlet. For friction modeling, surface roughness values of 0.005 and 0.03 were used for the intake and exhaust, respectively. These values were based on recommendations from Amesim and depend on the material properties of the respective surfaces.

In the demo model, see Figure 3.3, a manifold from the IFP-engine library was used. However, when using the CFD1D library, no predefined component representing a manifold was available. Therefore it was modeled using straight and curved pipes as shown in Figure 3.4 marked "INTAKE MANIFOLD" and "EXHAUST MANIFOLD". This approach of modeling the manifolds was inspired by another demo file available in the CFD1D library documentation.

Turbocharger

When using the predefined compressor component available in the CFD1D library, it calculates the pressure ratio and mass flow from an imported compressor map as described in Section 3.2.5. Amesim offers a couple compressor maps in the demo files, however, none of them were well adapted for the two cylinder 1 liter engine modeled in this project. In most cases, the compressor map was designed for a four cylinder engine meaning it was not scaled accurately for the two-cylinder engine, Baseline model. This resulted in unsteady flow and either surge or choke could occur in the compressor. An example of a compressor with surge is shown in Figure 3.5.

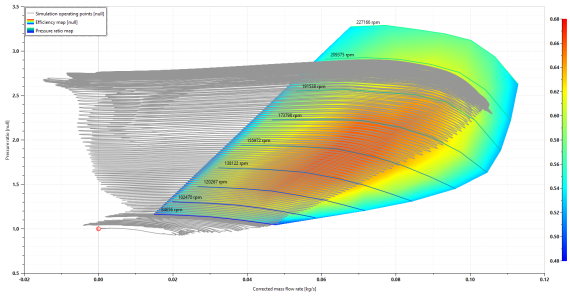

Figure 3.5: Surge compressor map

Without suitable compressor maps, the solution became to rescale an already existing one. This was achieved by reducing the efficiency making both the flow and the pressure ratio slightly lower.

The wastegate obtained from the demo file was placed in connection to the turbine. With an absolute pressure target downstream of the compressor, a controller operates the wastegate to the desired value.

Combustion cylinders

There are two combustion cylinders in the Baseline engine with a total cylinder displacement volume of 1 liter. In the list below, some of their main characteristics are listed.

- Bore = 83 mm
- Stroke = 83 mm
- Connecting rod length = 150 mm
- Compression ratio = 9

The two cylinders are phased 360 degrees. The spark timing of the engine was set to 10 CAD BTDC, however some variations to find the MBT curve was tested, see Chapter 4. In Table 3.2 the parameters related to burn duration are shown. When comparing these to the literature, see Section 3.2.2, both the combustion duration and CA50 are similar which increases the models validity.
The valve lift profiles were originally taken from the default files available in Amesim. These were then phased to achieve a good performance of the engine. To customize the valve lift profiles to the Baseline model, they were modified by making them both longer and shorter. It was also experimented with the Miller cycle, however, as it took longer than expected to utilize the positive effects of that method, it was decided that this was left

Parameter	Value [°CA]
CA05	357.2
CA50	369.9
CA90	383.7
Burn duration	26.5

Table 3.2: Combustion Angles

outside the scope of the project. In Figure 3.6, the final valve lift profiles that originated from the default files is shown.

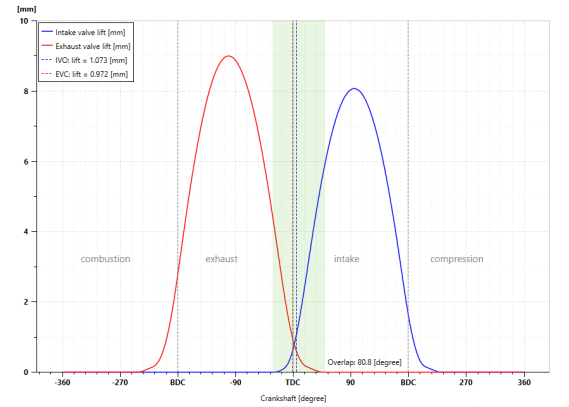

Figure 3.6: Valve lift profiles

Fuel system

As seen in Figure 3.4, a direct injection fuel system is used. The injector is controlled by injection timing, mass flow rate and injection duration. The mass of fuel is decided by the injection duration that is controlled by a controller that aims to hold the air/fuel mixture stoichiometric (lambda 1). If there is a high boost leading to more air in the cylinder, the injection duration gets longer to sustain a stoichiometric air/fuel mixture.

The fuel properties and what type of fuel that was chosen in Amesim can be seen in Table 3.3.

Lower heating value	44109 [kJ/kg]
Fuel type	ENG_GASOLINE_UNLEADED
Stoichiometric air/fuel ratio (AFR)	14.2341

Table 3.3: Fuel properties

3.3.2 Olshammar engine

The Olshammar engine, Figure 3.7, is modeled based on the Baseline engine, with an added exhaust cylinder and with a custom-made valve configuration to simulate the exhaust cylinder without intake and exhaust valves, see Figure 3.8. The exhaust runners from the combustion cylinders are connected to the modified exhaust cylinder, which then feeds the turbine with exhaust gas.

The Olshammar engine is, as earlier mentioned, modeled from the Baseline model. Most components, parameters and submodels are the same in the engine to ensure that the comparison between them depends on the key concepts of the Olshammar engine and not on for example turbocharging or manifold modeling. The differences in respective components for the Olshammar compared to the Baseline engine are described more in detail below.

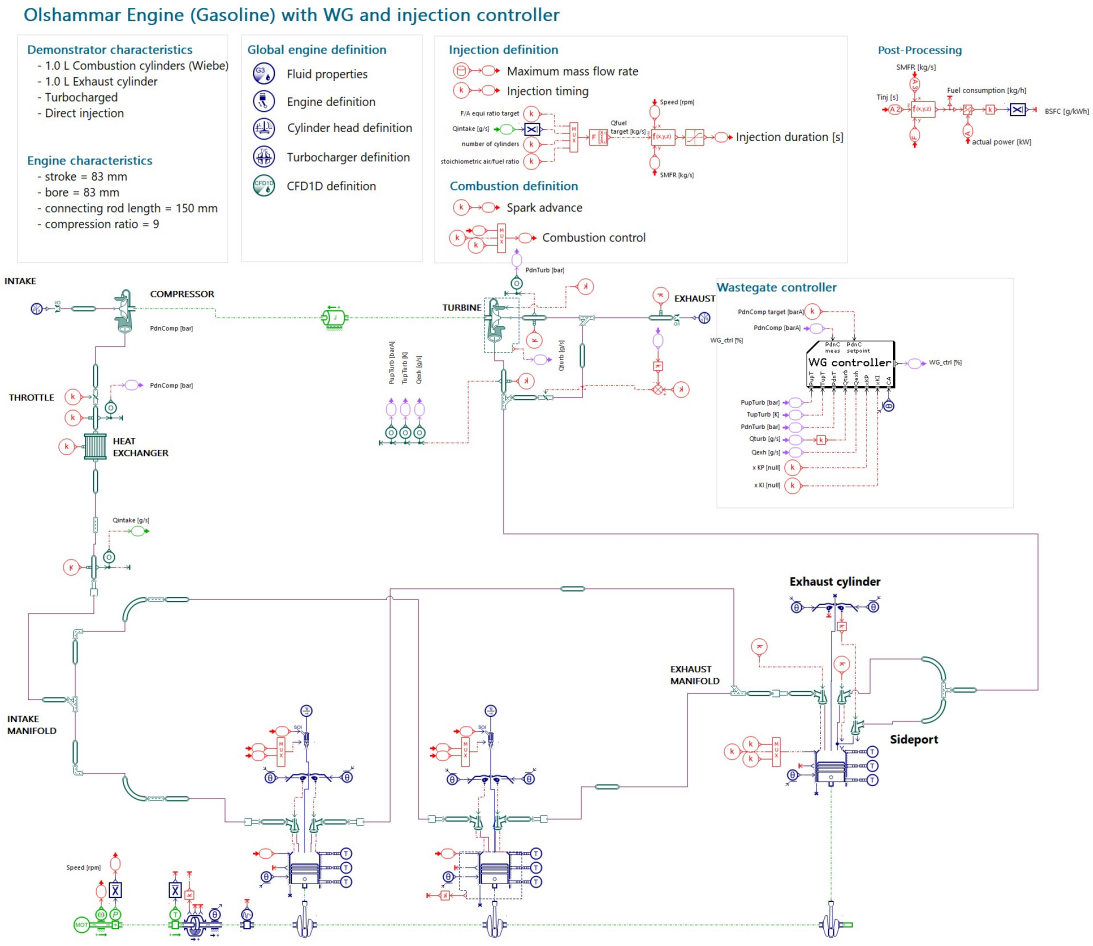

Figure 3.7: Olshammar Engine

Exhaust cylinder

As described in Chapter 2.1.3, the exhaust cylinder in the Olshammar engine has neither any combustion or valves (except sideport). However, Amesim does not provide any cylinder adapted for this purpose. A normal combustion cylinder was therefore used as the exhaust cylinder. To avoid combustion, a flow plug was placed instead of a fuel injector, resulting in no added fuel to the cylinder. To further reduce the risk of combustion, the combustion efficiency was set to 0. In order for the intake gases to enter and the exhaust gases to leave the cylinder, valves were needed. To model a cylinder without valves, a constant lift was applied to the valves, and by setting that lift high (1 meter), the valves are constantly open and affects the flow and combustion minimally.

The key different between the Olshammar and the Baseline engine lies within the exhaust cylinder that in this model has a stroke of 90 mm and a bore of 120 mm. The principle of having an additional exhaust cylinder without combustion is described in Section 2.2.6. The timing of the exhaust cylinder is made such that when a pulse from one combustion cylinder comes, expansion occurs where the pressure pulse helps pushing the piston down, adding torque to the crankshaft. When the piston moves up, the pressure from the combustion cylinders is smaller which means less resistance. This happens because a portion of the exhaust gas has already passed on to the turbine inlet (since there is no exhaust valve). In this way, positive work can be extracted from the exhaust gases in the exhaust cylinder.

Sideport

By placing an additional valve in the exhaust cylinder, it is possible to have even more control of the exhaust gases in the engine [15]. The approach to model this in Amesim is by adding an additional exhaust valve in the cylinder head, see configuration in Figure 3.8. The core idea is to have the extra valve closed when the gases expands in the cylinder, leading to a higher pressure on the piston which can extract work. When the piston reach BDC, the exhaust valve is opened which increases the area for the gases to flow out through. This is achieved by having a valve lift profile, see Figure 3.9 where the valve lift profile is plotted against the exhaust cylinder volume. As a result, the pressure in the exhaust cylinder is reduced faster leading to less resistant for the piston when moving towards TDC and therefore reduced pumping losses.

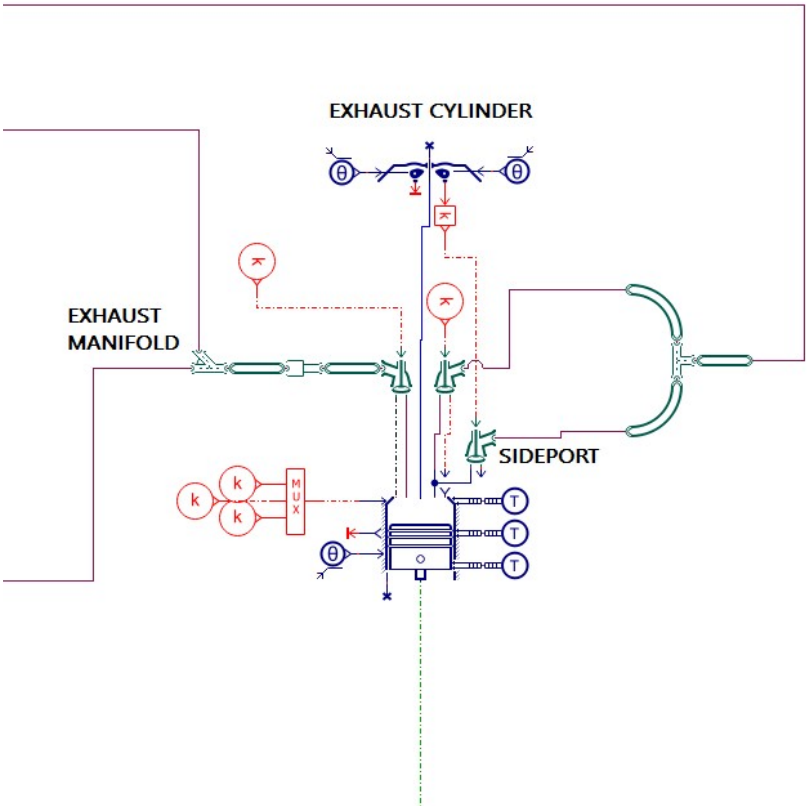

Figure 3.8: Exhaust cylinder with sideport

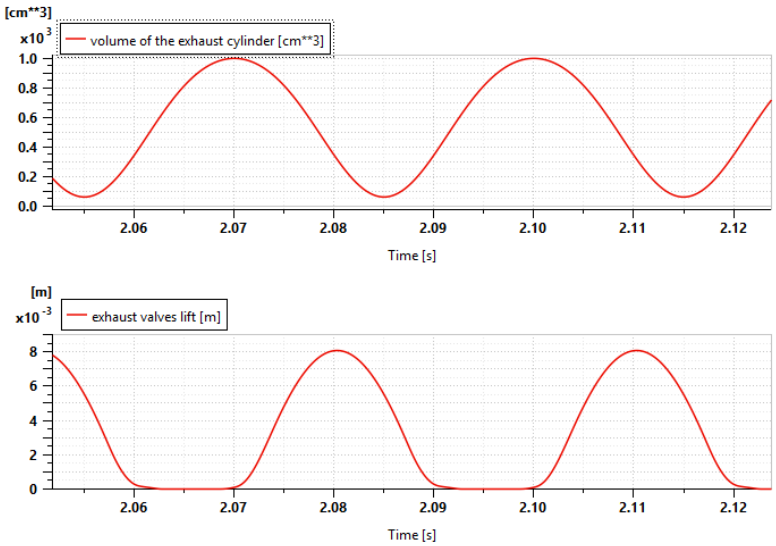

Figure 3.9: Valve lift for exhaust cylinder and sideport

3.4 Optimization

With established models, optimization was the next step in the process. The optimization is done using different studies in Amesim. The studies of consideration in this project were batch runs, design of experiments (DOE) and the inbuilt optimization tool which uses a generative algorithm to find the optimal solution based on user defined criteria. While the inbuilt optimization tool could be powerful, only a few parameters could be optimized at a time because of limitations in computational power, restricted by the number of threads on the computer. Therefore batch runs and DOE were the main methods for the optimization since they offered better possibilities in terms of control.

Optimizing systems with many parameters can be very difficult. The best would be to optimize all parameters at the same time in a large optimization, so later optimization is independent on earlier optimization. However, this requires huge computational resources. This is a trade off, computational power versus how many parameters that is optimized at a time.

The optimization started in an unstructured way. In order to get the baseline model to run properly and to be as robust as possible, a lot of parameters had to be tuned roughly. For example the spark ignition had to be somewhere before TDC and the intake system and turbocharger needed a lot of tuning to make the flow good enough to avoid crashes for small changes in related parameters.

Once a model that was robust enough to run when varying parameters in the model was achieved, the iterative optimization could start. The simulations were performed for 1000-6000 rpm. While all the engine speeds were covered in order to establish sufficient and reasonable values of the entire range, the parameters were set so that best performance was achieved at 2000 and 3000 rpm. To measure the performance of the models during optimization, torque, BP and BSFC were used. A balance between the parameters was also of interest in the end, to achieve a solid combination of brake fuel conversion efficiency and performance.

In order to keep some structure when optimizing the engines, subsystems of the engine were optimized one at a time. This also reduced the number of parameters meaning the computational power available was enough. The subsystems were the intake system, exhaust system, the combustion cylinders, the turbocharger and for the Olshammar model, the exhaust cylinder with sideport. The optimization was carried out in this order.

The Olshammar engine was modeled based on the already optimized baseline engine. Therefore, the intake system, combustion cylinders and turbocharger could remain the same while the exhaust system and the exhaust cylinder had to be re-optimized.

3.5 Timestep and tolerance analysis

To achieve results independent on the timestep and tolerance in the model, a timestep and tolerance analysis were performed. Table 3.4 shows the performance values of the Olshammar engine without sideport, running at 3000 rpm and a timestep of **T/5000**. The values in Table 3.4 show how dependent the solution is on the set tolerance, in order for the solution to reach convergence. The timestep under these conditions did not affect the outcome of the result and could therefore be fixed since the tolerance rather then the timestep defines the convergence of the system.

Tolerance	Torque	Brake Power	BSFC
0.01	112.2	35.2	254
0.001	123.5	39.8	234.7
0.0001	124.2	39.1	233.1
0.00001	124.2	39.1	233.1

Table 3.4: Timestep analysis.

With **Tolerance = 0.0001** based on the results in Table 3.4, and the same engine configuration and operation point as above, Figure 3.10 shows the dependence of timestep in terms of pressure-volume diagrams for one of the two combustion cylinders, in range from **T/100** to **T/10000**. A final value of **T/5000** was chosen for calculations of indicated values, where higher accuracy is needed, whereas a timestep of **T/100** with tolerance of **0.0001** was used when extracting converged values from the simulations as seen in Table 3.4.

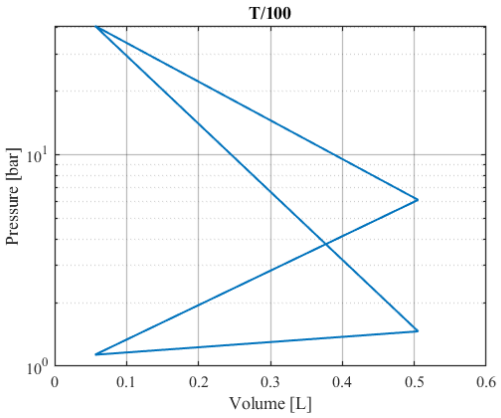

(a) T/100

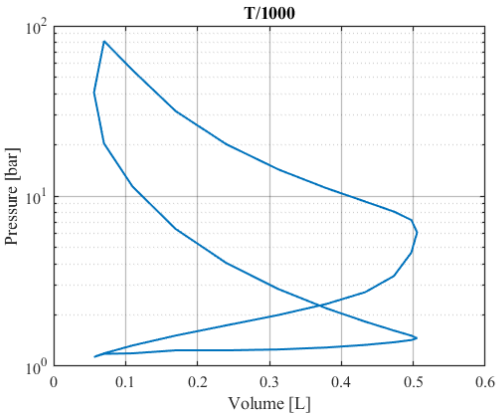

(d) T/1000

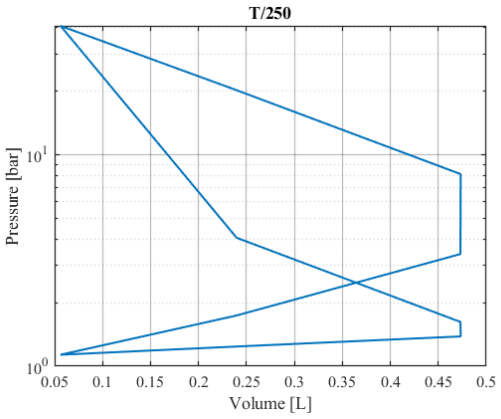

(b) T/250

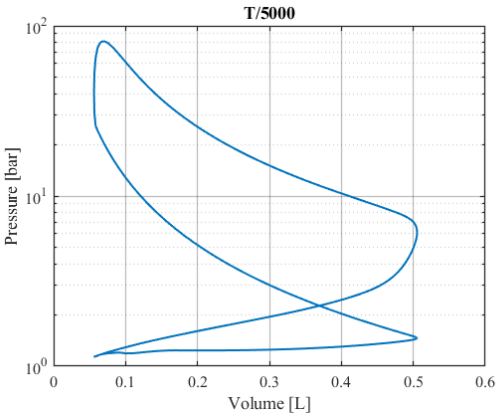

(e) T/5000

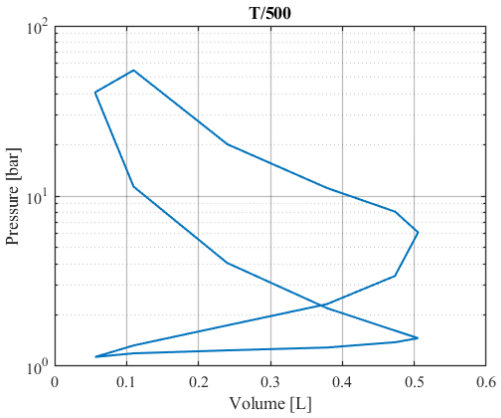

(c) T/500

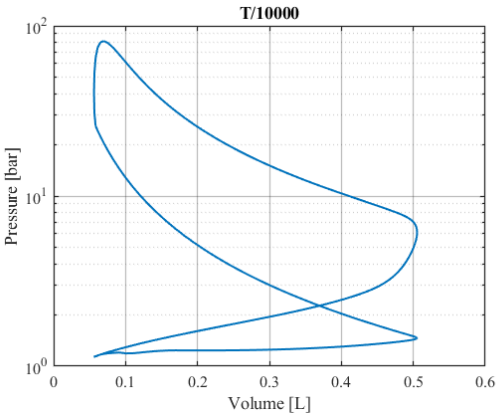

(f) T/10000

Figure 3.10: Timestep analysis of PV diagram of combustion cylinder

3.6 Knock analysis

As described in Section 2.2.7, knock can cause severe damage to the engine and must therefore be taken into account. While the aim of the engine modeling is to reduce fuel consumption (BSFC), not using knock as a limit might lead to a model with an unreasonably high performance compared to what a real world engine can achieve without knocking. As described in the theoretical background Section 2.2.7, too high temperature and pressure can cause a self ignition in the end gases leading to knock. To determine whether knock occur in the model, Amesim's built in knock detection function is used which provides the output parameter "BMF when knock detected". As mentioned in the knock modeling Section (3.2.3), the limit for when knock is considered to occur in the end gases is set to 85% mass fraction burnt. In Figure 3.11, the BMF knock detected is shown for 1000-6000 rpm with a spark ignition of 10 CAD BTDC.

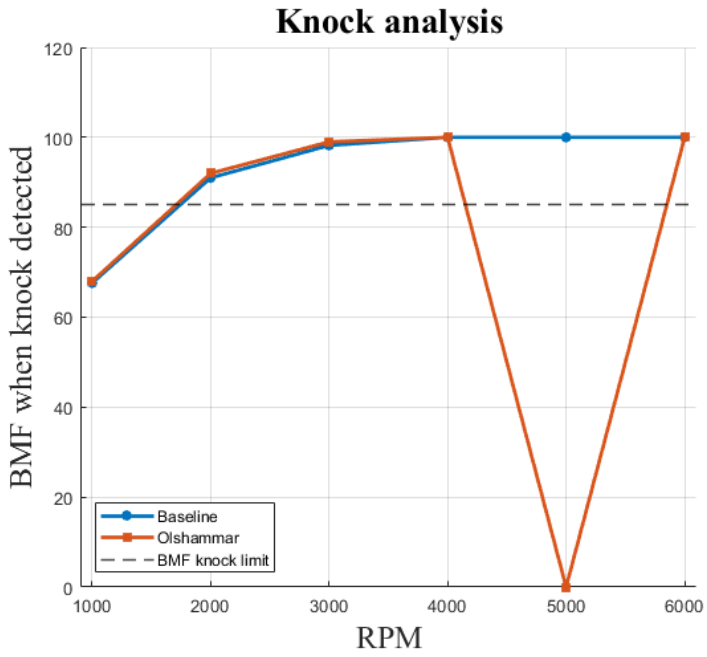

Figure 3.11: BMF when knock detected

Note that the curves are very similar for the Baseline and Olshammar model. There is an exception for the Olshammar engine at 5000 rpm where the BMF value is 0. This suggests that the engine is very sensitive and knocks heavily in these conditions. However, no other value indicates that the model is knocking. The peak pressure does not increase and the performance is not significantly better than for other values. See Table 3.5 for a comparison between a non knocking and a knocking spark ignition, where a spark timing of -20° indicate no knock with a higher maximum pressure than what a spark timing of -10° is showing.

Spark timing [°CA]	Torque [Nm]	BP [kW]	BSFC [g/kwh]	Max Press. [bar]	BMF knock
-10	102.5	53.6	272.0	80.0	0.00
-20	101.7	53.1	274.4	99.1	0.94

Table 3.5: Engine performance at 5000 rpm for selected spark timings

In Figure 3.11, both the Olshammar and the Baseline model fall below the 85% threshold for knock at 1000 rpm. It can be mitigated by retarding the spark timing. By retarding it from 10 CAD BTDC to 5 CAD ATDC both the models reach the knock threshold (Baseline 85.2 %, Olshammar 88.0 %). Similarly as the knocking case at 5000 rpm (Table 3.5), no significant increase in performance is seen for the simulations that knocks. This lies within how the knock model work. It does not model knock but rather monitor the combustion and evaluates the knock tendency, meaning that no knocking behavior is modeled. Because of this, knock should not be seen as a major limitation but rather a way to confirm that the models are somewhere around the reality. It is also worth to note that modeling knock is advanced and have big uncertainties and therefore should be used only as a guideline.

3.7 Validation

The validation targeted a study of a five-stroke engine, performed by Noga.M and Sendyka.B in 2013 [12]. The study was conducted using a four-stroke engine of 1.984 dm^3 with a maximum power of 147 kW. A turbocharger of model KP39 by Borg Warner was used in the tests. Test runs of the four-stroke engine was first performed, before rebuilding it to a five-stroke engine. It is the values of the four-stroke engine which are used to validate the Baseline model. The values of the validation are shown in Figure 3.12, where torque, BP and BSFC for a 1 liter engine configuration are being compared. The parameter of greatest interest for the validation is BSFC, which is reflected in Table 3.6, where the accuracy of BSFC is in range of $\pm$ 0-5 % when comparing the baseline with the study by Noga M. et al. According to Heywood (2019), the SI-engines with the lowest BSFC have typical values around 235 g/kWh, which is in the same range as the lowest values in the validation of the Baseline engine[4].

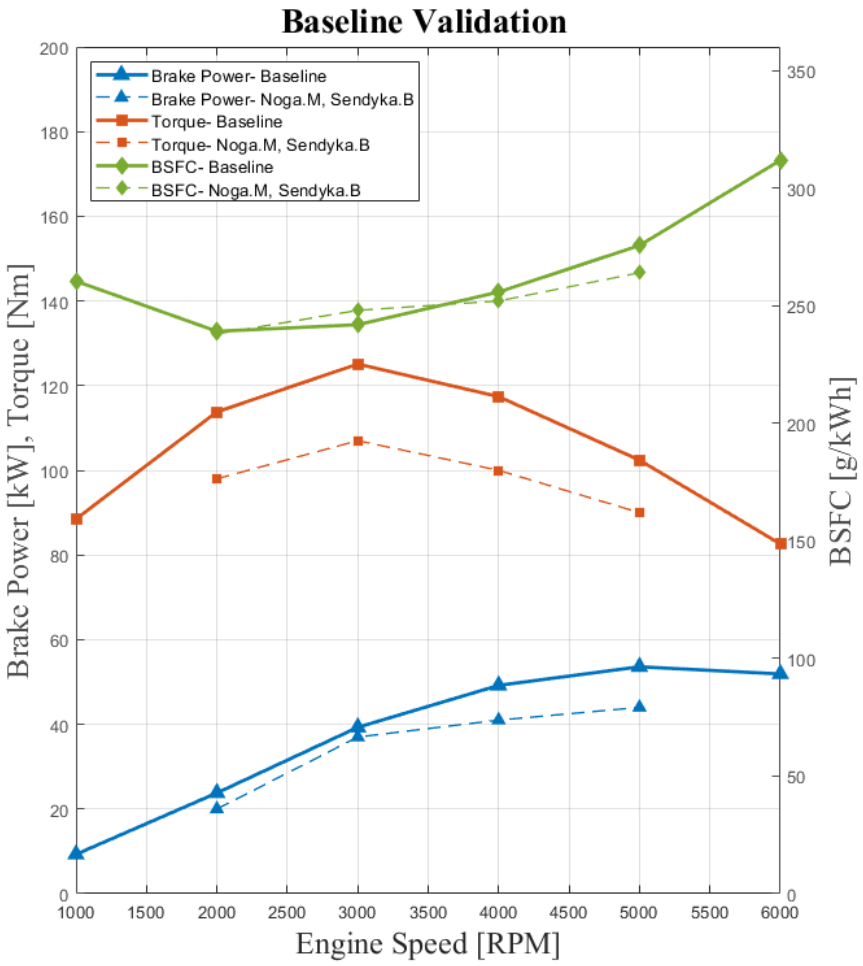

Figure 3.12: Validation of Baseline Engine

RPM	Torque% diff	Brake power% diff	BSFC% diff
2000	16.1	19	0.5
3000	16.9	6.2	-2.5
4000	17.4	20	1.5
5000	13.8	21.8	4.4

Table 3.6: Validation accuracy for baseline compared to literature engine

By validating the Baseline, a solid foundation was built for the work to continue on in terms of the Olshammar engine which is based on the Baseline model.

This page intentionally left blank.

4
Results

After completing the engine models, their relative performance was evaluated to determine whether the Olshammar engine provides an improvement compared to the baseline configuration. In addition, different variations of the Olshammar engine were examined more in detail, including the influence of the sideport, the timing of the exhaust cylinder, and the power contribution of the exhaust cylinder compared to the combustion cylinders.

4.1 Performance Comparison

The following comparisons are made for the different engine configurations, operating in engine speed range of 1000-6000 rpm, under wide open throttle (WOT) conditions. The comparisons were mainly aimed at analyzing variations in BSFC across the different configurations by selecting operating points for the models that corresponds to the same torque.

Olshammar engine without sideport compared to Baseline engine

Without the sideport on the exhaust cylinder, Figure 4.1a show that the Olshammar engine reduce BSFC in the range of 2000-4000 rpm compared to the Baseline. At 1000 and 6000 rpm, BSFC was on the other hand increased. The change in percentage is shown in Figure 4.1b, where the Olshammar engine without sideport achieves lowest BSFC compared to the baseline at 3000 rpm. The fuel conversion efficiency of the baseline at 3000 rpm is $\eta_f = 33.7\%$, compared to $\eta_f = 35.0\%$ for the Olshammar.

Olshammar engine with sideport compared to Baseline engine

When comparing the performance of the Olshammar engine with an additional sideport to the Baseline engine, similar results to the ones presented in Figure 4.1a were seen. The results are shown in Figure 4.2, where the main difference is seen at 5000 rpm, where the addition of the sideport decrease BSFC. The result of the sideport is further presented in Section: Effect of sideport in Olshammar engine. The fuel conversion efficiency of the Olshammar engine with sideport is $\eta_f = 35.2\%$ at 3000 rpm.

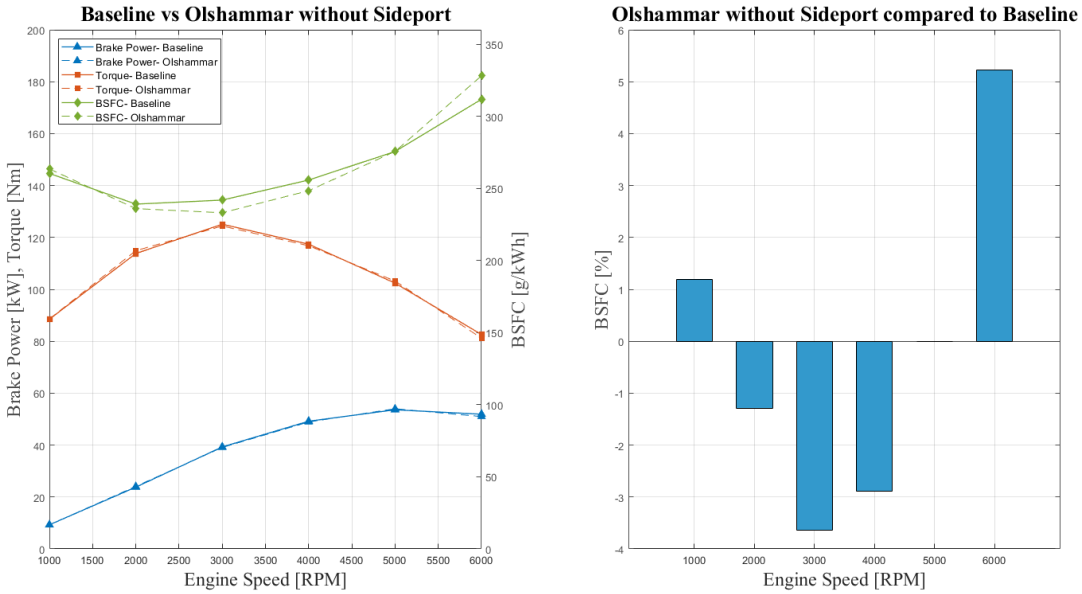

(a) **(b)**

Figure 4.1: Olshammar engine without sideport compared to Baseline

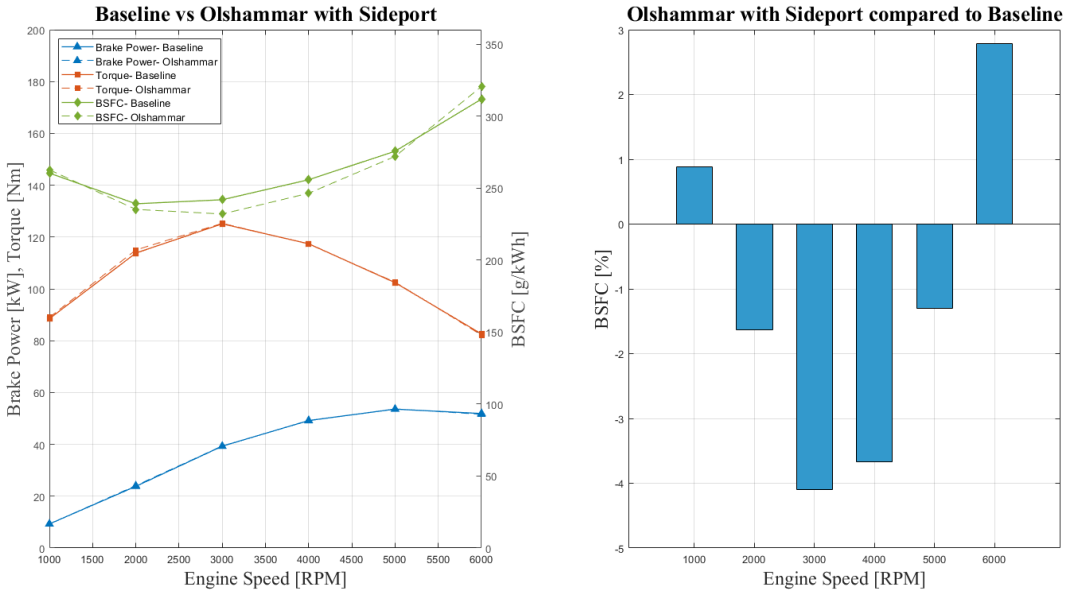

(a) **(b)**

Figure 4.2: Olshammar engine with sideport compared to Baseline

Effect of sideport in the Olshammar engine

Comparing the Olshammar engine with and without the addition of the sideport, Figure 4.3, show that there is a relation between decrease of BSFC and increased engine speed when the sideport is added. Table 4.1 shows the boost pressure of the engine. With close to the same boost pressure value of the configuration with sideport and without, Table 4.1 ensure that the improved BSFC of the sideport configuration is not due to the boost pressure difference compared to the configuration without sideport.

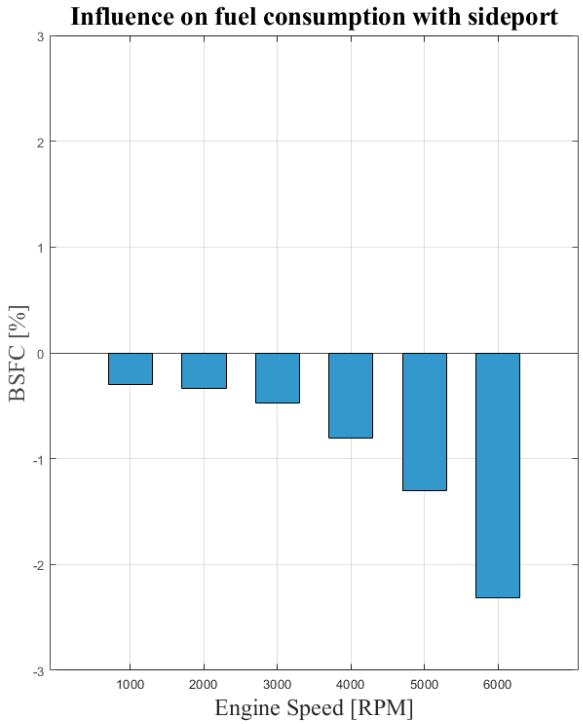

Figure 4.3: Influence on fuel consumption with sideport

RPM	Baseline [bar]	Olshammar with sideport [bar]	Olshammar without sideport [bar]
1000	1.15	1.17	1.17
2000	1.39	1.36	1.38
3000	1.55	1.51	1.49
4000	1.73	1.64	1.65
5000	1.88	1.81	1.85
6000	1.95	1.96	2.00

Table 4.1: Comparison of absolute boost values

4.2 Indicated values of combustion cylinders and exhaust cylinder

To be able to capture the contribution of the exhaust cylinder in terms of the overall performance of the engine, the indicated values of each cylinder had to be compared. The following figures illustrate the operating cycles of the HP combustion cylinders and the LP exhaust cylinder for the Olshammar engine configuration with sideport. The engine operates at 1000-6000 rpm under wide-open throttle (WOT) conditions.

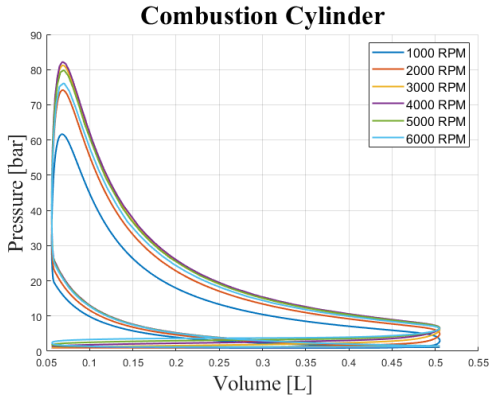

(a) PV diagram of Combustion Cylinder

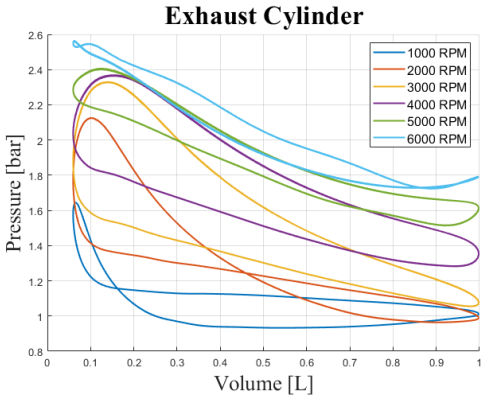

(b) PV diagram of Exhaust Cylinder

Table 4.2 show the contribution of the exhaust cylinder in terms of IMEP and indicated power.

RPM	IMEP [Bar]	Ind. Power [kW]
1000	13.8	10.3
2000	17.4	26.0
3000	18.7	42.0
4000	18.3	54.8
5000	17.3	64.8
6000	15.7	70.6

(a) Total Ind. Values of Combustion cylinders

RPM	IMEP [Bar]	Ind. Power [kW]
1000	-0.2	-0.16
2000	0.18	0.28
3000	0.73	1.7
4000	0.70	2.2
5000	0.31	1.2
6000	-0.16	-0.76

(b) Ind. Values of Exhaust cylinder

Table 4.2: Comparison of indicated values between combustion and exhaust cylinders.

4.3 Maximum Brake Torque

For the Olshammar model with sideport, the maximum brake torque (MBT) curve under WOT conditions for engine speeds of 1000-6000 rpm are shown in Figure 4.5. A spark ignition timing of 10 CAD BTDC (-10) provide MBT for engine speed of 1000-4000 rpm, and a more advanced spark ignition of 15 CAD BTDC result in higher torque for engine speed of 5000-6000 rpm.

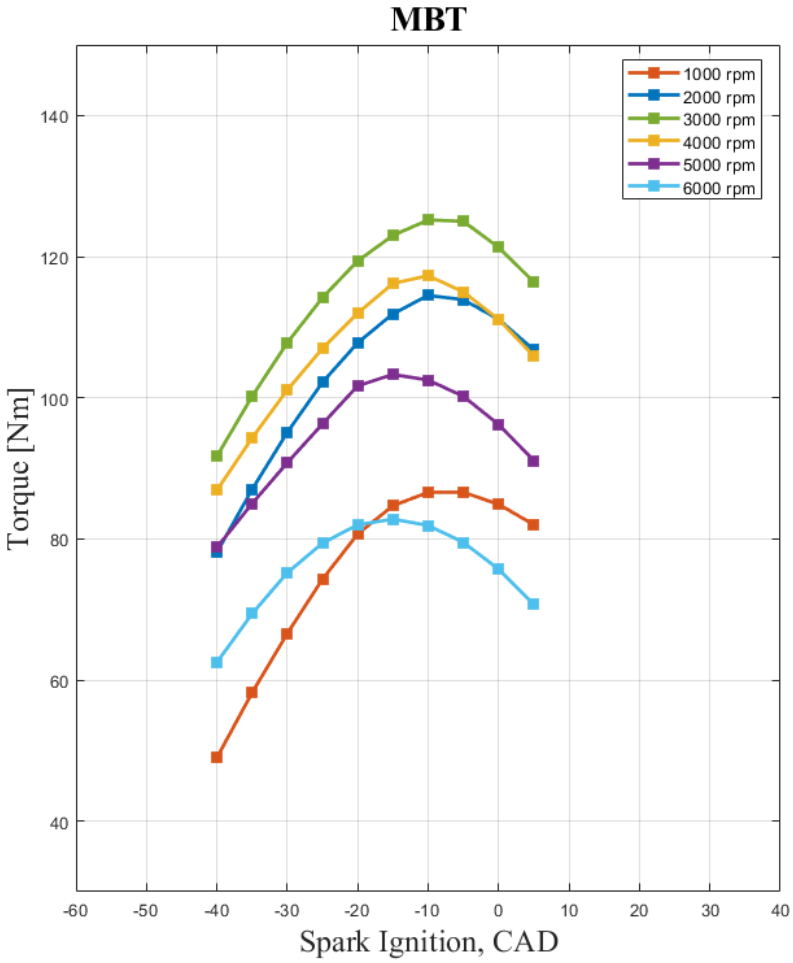

Figure 4.5: Maximum Brake Torque

4.4 Timing of exhaust cylinder in relation to combustion cylinders

By changing the offset of the exhaust cylinder in relation to the combustion cylinders, Figure 4.6 visualize the effect that the offset have on brake torque, brake power and BSFC. In the standard configuration when offset is 0, the exhaust cylinder is phased 180 CAD to the combustion cylinders. The effect of the offset is mainly seen at the higher engine speed of 6000 rpm, where the BSFC is reduced to 311 g/kWh with an offset of 20 CAD, compared to 320 g/kWh in the standard configuration.

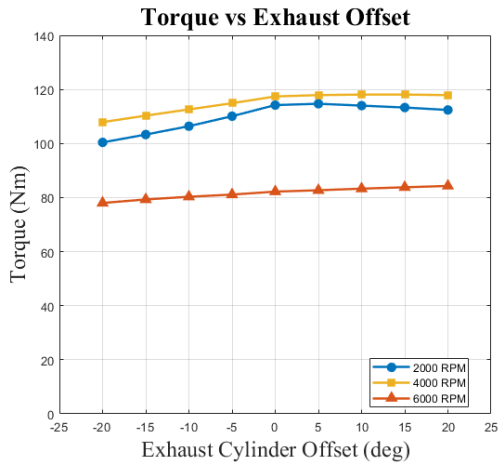

(a) Torque vs exhaust offset

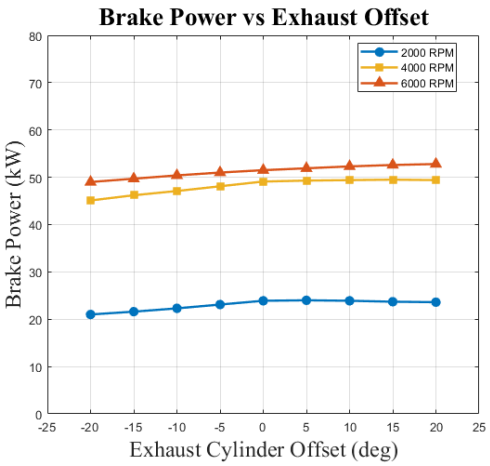

(b) Brake power vs exhaust offset

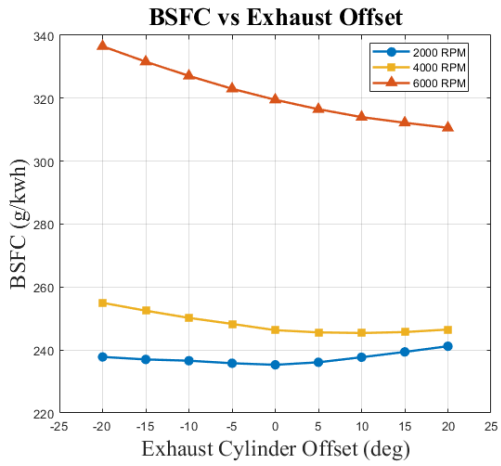

(c) BSFC vs exhaust offset

Figure 4.6: Exhaust cylinder offset variation.

4.5 Variation of bore and stroke of the exhaust cylinder

The geometry of the exhaust cylinder, with respect to bore and stroke, shows a varying effect on the overall performance of the engine according to Figure 4.7 and 4.8. With operating points of 2000-3000 rpm where the engine is optimized for, the results show that for 2000 rpm, a shorter stroke of 90mm and a bore of 120mm result in lowest BSFC and highest torque. For 3000 rpm however, the lowest BSFC was still achieved at a stroke of 90mm and a bore of 120mm, but the torque increased on the other hand with a larger bore.

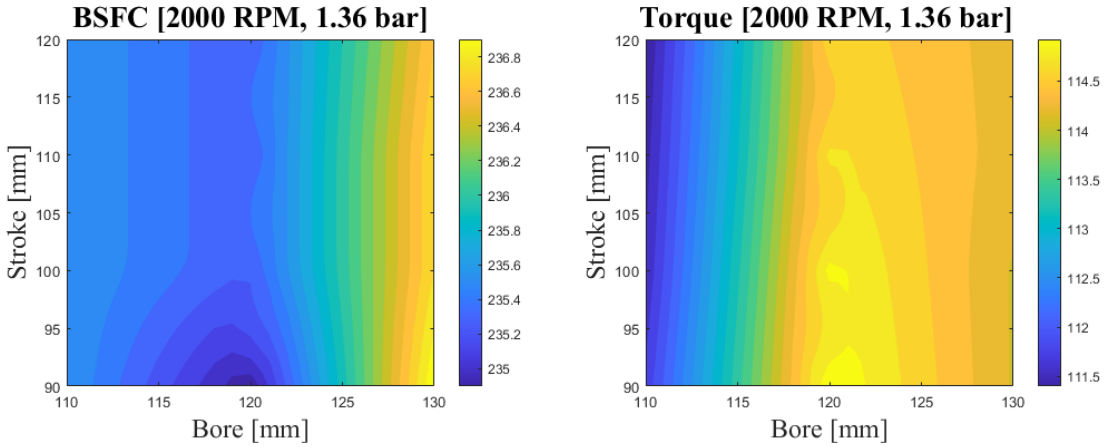

(a) **(b)**

Figure 4.7: Variation of bore and stroke at 2000 rpm.

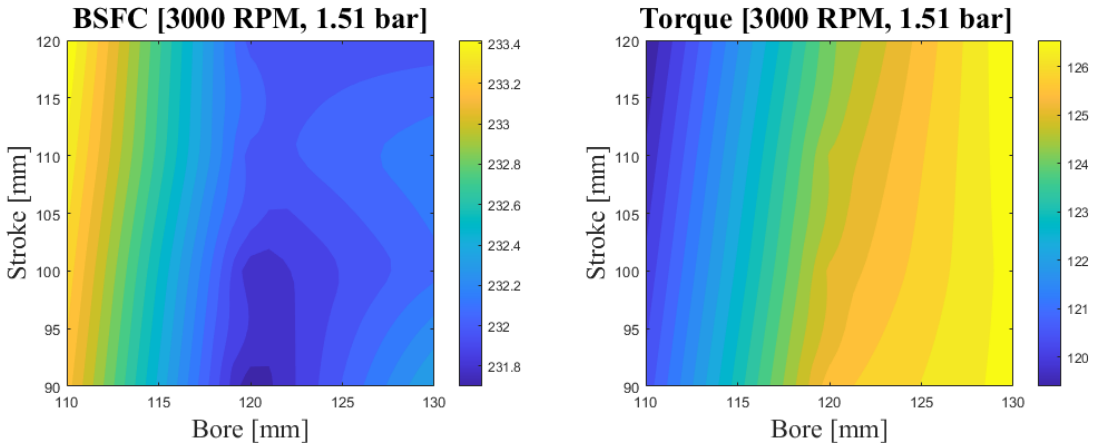

(a) **(b)**

Figure 4.8: Variation of bore and stroke at 3000 rpm.

4.6 Pressure pulses in exhaust

This section presents the behavior of the flow in the exhaust system of the engines, and more specifically how the efficiency of the turbine and compressor are effected for the baseline and Olshammar engine models.

The pulses of the pressure and mass flow rate in the exhaust system, for different engine speeds prior to the turbine, are presented in Figures B.1 and B.2 in the Appendix. As the engine speed is increased, the curves for both the pressure and mass flow rate is lifted in the region between the peaks of the pulses for the Olshammar engine compared to the Baseline. In other words, the pressure and the mass flow into the turbine becomes more even.

In Appendix, Figure B.3 and B.4, it is harder to draw any conclusions from the graphs whether the efficiency for the turbine and compressor differ between the Olshammar and the Baseline model. For 6000 rpm the efficiency do not drop as low for the Olshammar compared to the Baseline model. However, the difference between the Olshammar and Baseline models efficiency for other rpm are not unambiguous.

This page intentionally left blank.

5
Discussion

In this chapter, the results are discussed in greater depth and related to the research questions presented in Section 1.3.

5.1 Analysis of the results and the contribution of exhaust cylinder

In terms of performance, the Olshammar engine show a reduced BSFC at 2000-5000 rpm for the sideport configuration when compared to the Baseline engine. The increase of performance is a result of the additional contribution of power that the exhaust cylinder contributes with, seen in Table 4.2b. Even though the exhaust cylinder provides additional power, the heat-losses of the additional 5th stroke would need further evaluation. According to Stuart, K. et al. (2017), the heat losses of the 5th stroke can be around 41% [20]. This would need further evaluation in the model, but it could give an early indication that the heat losses can be larger than they currently are.

The addition of the sideport allows the pressure to be released quicker during the exhaust stroke by increasing the area for the gases to flow out through. As a result, during the exhaust stroke, the work done by the exhaust gas on the piston is reduced as it ascends toward TDC, which effectively reduces pumping losses. Further, the simulations showed that the sideport reduced BSFC more as the engine speed and boost pressure increased. The fact that the sideport showed more improvement for higher boost pressure could possibly mean that a larger engine, operating at higher boost, could benefit to a greater extent from the sideport compared to the engine model in this thesis. Worth to note is that the sideport was modeled using a valve lift profile, see Section 3.3.2, while it in the conceptual idea presented by Olshammar [15] is described as a hole in the cylinder wall to remove the need of a camshaft. A consequence of this is that the Olshammar model in this project will get better results than it would with the sideport as a hole in the cylinder wall due to the optimized valve lift profile.

In general, the torque curve for a boosted engine is usually flatter over the engine speed than what Figure 4.1a show, but due to how the comparison was performed, the maximum boost pressure is limited, and therefore the torque at higher engine speed is slightly decreased [19]. This explains why the torque curves obtained from the simulations have a larger decline for higher rpm.

An aspect to consider when evaluating the result of the MBT curve is that the boost

pressure is limited with the wastegate controller, to allow a fair comparison between the models. Since a more retarded spark timing highly influence the exhaust gas temperature according to Stone. R (2014), the boost pressure for a more retarded spark could in theory be higher if the boost pressure was not limited by the wastegate [19]. This would result in a different MBT curve due to possibly higher torque as a result of greater turbine work [19].

5.2 Sensitivity analysis

Despite a lot of efforts making the engine models as representative for a real engine as possible, they are still only models of the real world. That is very important to have in mind. Therefore, this sensitivity analysis of parameters influence on the results (engine performance) and model robustness is carried out.

In the start of the project, the model robustness were a main issue. In particular when it came to modeling the gas flow using the CFD1D library. Changing lengths or diameters anywhere in the intake or exhaust system could result in computational errors in the pipe downstream of the compressor. By tuning the compressor, intake and exhaust system, a more robust system was achieved where small changes did not result in computational errors anymore. However, it is still clear that the gas flow modeling has a huge impact on the model robustness.

Connecting to the gas flow modeling, the turbocharger is important both for the model robustness and the influence on the engine performance. The parameter with the main influence was the turbocharger inertia, see the inertia between the compressor and turbine in Figure 3.1. A too low inertia made the compressor very sensitive to mass flow variations resulting in backflow and surge. A good example of this is the compressor map seen in Figure 3.5. If the inertia was too high, the efficiency of the turbocharger dropped significantly and was not able to generate any boost. The balance between too high and low inertia was crucial and had to be tuned carefully.

For the combustion modeling, the Wiebe function was used. As described in Section 3.2.2 the shape of the Wiebe function can be changed with the parameters a and m (named a and f in Amesim). These two parameter had a big influence on the whole combustion regarding multiple aspects. The performance of the model changed drastically and important characteristics such as burn duration, cylinder pressure and cylinder temperature were affected. The parameters had to be tuned with care to achieve a reasonable combustion. The main output that was studied here was the burn duration.

5.3 Modeling internal combustion engines in Amesim

In the research question, see Section 1.3, one of the question is "What are the advantages and disadvantages of Amesim in terms of modeling internal combustion engines?". Before any conclusion is drawn, it is important to note that this is the subjective experience of the thesis workers and that they had no prior experience with modeling in Amesim.

Even though there where three sessions with technical experts from Siemens and Volupe, most of the time the learning process and troubleshooting had to be done without help or support.

The main advantage experienced in Amesim was the user interface. It was easy to get started in the program and to understand the different workbenches (sketch, submodels, parameters, simulation). For example the click and drag function in sketch mode made it easy to import and connect different components, making it possible to build up models fast. The integrated help function in Amesim was also highly beneficial. It provided direct access to the documentation of each selected component, including the underlying physical models and available parameters and submodels. As a result, the modeling of the engines were straight forward considering the prerequisites. Another advantage of the usability was related to the creation of plots, where the parameter of interest was dragged and dropped in the model. The possibility of making pre-defined plots that updates after a new simulation was also time saving.

A challenge in Amesim for the thesis workers were that the program had to be learned independently and without supervisors. Despite efforts being made, no one at Chalmers with prior knowledge from simulating ICEs in Amesim similar to the one in this project was found. During the project it became evident that Amesim is not a software tool developed solely for combustion engine simulations. For example it was hard to have exact control over the combustion duration. The need for controllers to sustain a constant lambda value and boost pressure were also things that had to be modeled while it might would be expected to be integrated in components for a program made specifically for ICE modeling.

The biggest challenge was to model the gas flow with a turbocharger using the CFD1D library. Before tuning and optimizing it correctly, the difference of a few millimeters in a pipe length could make the entire simulation crash. Eventually, by optimizing pipes, intake manifold and compressor map, a stable flow could be achieved. However, this was very time consuming and there was not a lot of either documentation or demo files that could provide support on how to solve the problem with instability in the intake system. As for being a disadvantage for Amesim, it can be concluded that the CFD1D library is very sensitive for modeling combustion engines. It is worth noting that the IFP-engine library solves this problem, however not with the same accuracy in the gas flow modeling as the CFD1D library.

5.3.1 Comparison between Amesim and GT-Power

Since a part of this thesis also is about evaluating the possibility for Chalmers to replace GT-Power with Amesim for modeling and simulating ICE, a brief comparison is conducted that summarize the key differences between the two software's. The thesis workers experience in GT-Power is limited to a few weeks of optimizing an ICE in an earlier course at Chalmers. Therefore, the comparison can not be as in depth as would be desirable.

The industry leading software for modeling and simulating ICEs is GT-Power, created by Gamma Technologies. GT-Power is developed solely for combustion modeling which means it is tailored for this purpose. Compared to Amesim, the key advantage of GT-Power is the ease to use while still showing high level of detail combined with fast computations. In terms of achieving accurate ICE modeling in Amesim as previously discussed in Section 3.1, the IFP-Engine library is ideally combined with the CFD1D library. This achieve high accuracy of gas modeling, but with some following disadvantages. Table 5.1 explains the cons and pros of the IFP-Engine and CFD1D library compared to GT-Power when it comes to flow modeling.

	Amesim-CFD1D	**Amesim-IFP-Engine**	**GT Power**
Difficulty	High	Low	Low
Level of Detail	High	Low	High
Robustness	Low	High	High
Time Consumption	High	Low	Low

Table 5.1: Comparison of Amesim and GT-Power for gas flow simulation.

After using the programs as a beginner it is still clear that the differences in the programs can be connected to what they are developed for. Amesim is a platform where multiple subsystems can be imported or developed and then studied in a system context where subsystems work together. It can for example be for simulating entire powertrains in a vehicle, where an ICE can be a subsystem. GT-Power however aims to study only the ICE, that is the only thing it has been developed for. Because of this, computational factors such as solvers for gas flow in the engine, have been tailored for the specific challenges that the combustion engine comes with. It also allows the user to go a bit more into detail in the combustion modeling. Overall this makes GT-Power a more suitable choice simulating ICEs in depth and when the user needs to be in control of every little detail. The advantage with Amesim however is the more friendly user interface. The opportunity to integrate the ICE as a subsystem also makes it the clear choice over GT Power when simulating bigger systems.

5.4 Differences from earlier studies

Previous studies on the Olshammar engine have compared its performance to an equivalent baseline engine. In those studies, the operating point is decided by the boost pressure resulting in different brake torque, brake power and BSFC for the two engines. Meaning that the comparison were made under unequal operating conditions. The performance of the Olshammar engine was then evaluated both for BSFC and BP. In this thesis, the operating point is instead defined by the brake torque where the baseline and Olshammar model achieves the same brake torque by varying the boost pressure, enabling a fair comparison. By evaluating the BSFC at equal torque output, it becomes possible to determine which engine delivers the same power with the least amount of fuel input (lowest BSFC). To verify this, the injection duration was also examined to ensure that the more efficient engine indeed consumed less fuel, which was confirmed by the results (see Appendix, Figure A.1 and A.2).

Compared to earlier studies, this thesis treats lower boost pressure. There is one main reason for this. The exhaust gases produced from the engines were not sufficient for the turbocharger to reach as high boost pressures as earlier studies had used. This was especially true for low rpms where the maximum boost for 1000 and 2000 rpm were 1.15 and 1.39 respectively for the baseline engine. Both the study carried out by KTH [10] and FEV [21] reached higher boost pressures with a maximum of 3.5 bar for 1000 and 2000 rpm. The reason for this difference can probably be linked to the modeling of the turbocharger. KTH and FEV used GT-Power and while FEV does not state what kind of turbocharger model that was used, KTH used a simple turbocharger model. This thesis used a CFD1D turbocharger in Amesim which could be the reason for a lower boost pressure. It is also reasonable that it is harder to reach high boost pressure for lower rpm due to less energy in the exhaust gas, and this was also supported by observations. According to Westin (2005), scientific literature covering pressure ratios of higher than 3 (meaning absolute pressure of more than 3 bar) can not be found for passenger car sized SI engines[23]. The reason being these engines normally requires two-stage systems and are mainly using diesel as fuel.

When comparing the performance of the Olshammar versus the baseline engine for this thesis and the previous studies made by KTH and FEV, the results are quite different. They are visualized in Table 5.2 and highlights how the benefits regarding performance were smaller in this thesis in relation to the earlier studies. However, because of taking knock into account, the more realistic boost pressure and that the operational points for the Olshammar and the Baseline engine were the same when compared, the thesis workers would like to argue that the validity of these results are higher than for the earlier studies. This claim is further strengthened by the validation of the Baseline engine against another engine carried out in Section 3.7.

Study	**Average BSFC reduction**	**Average BP increase**	**Absolute pressure [bar]**	**RPM included**	**Reference**
FEV	7.8%	23.8%	3.5	2000-5000	Table 2.2
KTH	4%	5%	3.5	2000-6500	Section 2.1.4
This thesis	1.2%	0	1.17-1.96	1000-6000	Figure 4.2

Table 5.2: Relative change in performance for Olshammar compared to baseline engine for different studies

This page intentionally left blank.

6
Conclusion

With the use of Amesim, modeling of the Olshammar engine was successfully achieved. Through a simulation-based approach, the Olshammar engine was optimized for 2000-3000 rpm and validated against a real constructed four-stroke engine created by Noga.M et al. [12]. Designing turbocharged engines requires tuning of parameters such as compression ratio to prevent knock and ensuring a robust model. The results show that the Olshammar engine reduce fuel consumption, where the main contributing factors has proven to be the additional power gain of the expansion stroke in the exhaust cylinder, and also the reduced pumping losses as a result of the sideport. The average BSFC reduction is 1.2 % over the entire operating range of 1000-6000 rpm, with the largest BSFC reduction of approximately 4% obtained at 3000 rpm.

Chalmers explores alternatives to GT-Power for engine modeling since it's a rather expensive program, and this study emphasizes the potential of Amesim as a possible replacement for GT-Power in the future. The key reasons are the short learning curve due to well established demo-files, tutorials and a significant amount of documentation that describes the different parts in detail. The use of the IFP-Engine library is rather simple and is sufficient in most cases, but for a more detailed engine where higher accuracy of the flow is required, the CFD1D library is recommended. The main downside of Amesim in comparison to GT-power is the robustness of the system, where the CFD1D library showed to lack in robustness on occasion. In conclusion, Siemens Amesim would be a good replacement for GT-Power for the projects in the ICE course at Chalmers if only the IFP-Engine library was to be used. This would be beneficial for Chalmers economically, while the students would still reach the learning objectives in the ICE course.

A future recommendation for the Olshammar engine would be to look into systems where weight and space efficiency is not a primary concern, in comparison to for example automotive vehicles. This could include genset and marine applications. Further, it would thus involve modeling larger Olshammar engines that operates under higher boost pressure to a further extent show the potential of the concept compared to smaller engines, similar to the one modeled in this study. It would also be reasonable to explore options of alternative fuels where the exhaust gases contain more energy, as this could potentially increase efficiency and overall performance of the engine.

This page intentionally left blank.

Bibliography

[1] Siemens Amesim. *cfd1d_library*.

[2] Siemens Amesim. *ENGBMFWIEBE01V01 - combustion model with specified BMF, heat released or Wiebe laws*.

[3] "Five-stroke internal combustion engine". In: (Oct. 2001).

[4] John B Heywood. *Internal Combustion Engine Fundamentals*. 2nd. 2019. ISBN: 9781260116106.

[5] John B.. Heywood. *Internal combustion engine fundamentals*. McGraw-Hill Book Company, 1988, p. 930. ISBN: 007028637X.

[6] Peter Hiereth Hermann. Prenningen. *Chargint the Internal Combustion Engine*. Ed. by Helmut List. Powertrain, 2007.

[7] J.D. Naber and J.E. Johnson. *Alternative Fuels and Advanced Vehicle Technologies for Improved Environmental Performance*. 2014, pp. 197–224.

[8] A. Kéromnès et al. "Development and validation of a 5 stroke engine for range extenders application". In: *Energy Conversion and Management* 82 (June 2014), pp. 259–267. ISSN: 0196-8904. DOI: 10.1016/J.ENCONMAN.2014.03.025. https://www.sciencedirect.com/science/article/pii/S0196890414002179?via%3Dihub.

[9] Tie Li, Bin Wang, and Bin Zheng. "A comparison between Miller and five-stroke cycles for enabling deeply downsized, highly boosted, spark-ignition engines with ultra expansion". In: *Energy Conversion and Management* 123 (Sept. 2016), pp. 140–152. ISSN: 0196-8904. DOI: 10.1016/J.ENCONMAN.2016.06.038.

[10] Nachiketh Lingachari Acharya and Saurav Dasgupta. "Performance Investigation & Gas Exchange Assessment of Exhaust Piston-assisted Turbocharged Engine (EPTE)". In: (2021). https://usercontent.one/wp/www.olshammar.com/wp-content/uploads/2022/08/MasterThesisReport_MF225X_2021.pdf.

[11] Anthony J. Martyr and David R. Rogers. "The combustion process and combustion analysis". In: *Engine Testing* (2021), pp. 537–597. DOI: 10.1016/B978-0-12-821226-4.00016-4.

[12] Marcin Noga and Bronisław Sendyka. "NEW DESIGN OF THE FIVE-STROKE SI ENGINE". In: *Journal of KONES. Powertrain and Transport* 20.1 (Jan. 2013), pp. 239–246. ISSN: 1231-4005. DOI: 10.5604/12314005.1136161.

[13] Rafiu K Olalere et al. *Experimental study of combustion and emissions characteristics of low blend ratio of 2-methylfuran/ 2-methyltetrahyrofuran with gasoline in a DISI engine*. Tech. rep. 2024.

[14] Mats Olshammar. *Olshammar Engine & Nebula AB – Olshammar Engine & Abrasec*. 2025.
https://www.olshammar.com/.

[15] Mats Olshammar. *Patent specifikation*. 2019.
https://usercontent.one/wp/www.olshammar.com/wp-content/uploads/2022/08/SE541204.C2.pdf.

[16] Willard W Pulkrabek. *Engineering Fundamentals of the Internal Combustion Engine*. 2004.

[17] Joshi Sidharath. *5 STROKE ENGINE-A REVOLUTIONARY PATHWAY FOR EFFICIENT ENGINE PERFORMANCE*. Jan. 2017.
https://www.researchgate.net/publication/338233473_5_STROKE_ENGINE-A_REVOLUTIONARY_PATHWAY_FOR_EFFICIENT_ENGINE_PERFORMANCE.

[18] *Simcenter Amesim | Siemens Software*. 2025.
https://plm.sw.siemens.com/en-US/simcenter/systems-simulation/amesim/.

[19] Richard Stone. *Introduction to internal combustion engines*. 4th. 2014.

[20] Kurt Stuart, Terry Yan, and James Mathias. "Thermodynamic Analysis of a Five-Stroke Engine with Heat Transfer and Mass Loss". In: *SAE Technical Papers* 2017-March.March (Mar. 2017). ISSN: 01487191. DOI: 10.4271/2017-01-0633.
https://saemobilus.sae.org/papers/thermodynamic-analysis-a-five-stroke-engine-heat-transfer-mass-loss-2017-01-0633.

[21] Jia Sun. *GT-POWER SIMULATIONS OF OLSHAMMAR ENGINE*. Tech. rep. FEV Sverige AB, Oct. 2023.
www.olshammar.com.

[22] *The world's most powerful four-cylinder engine in series production, made in Affalterbach*. 2019.
https://media.mbusa.com/releases/release-6d7a68ca18d81680d3687d107907853e-the-worlds-most-powerful-four-cylinder-engine-in-series-production-made-in-affalterbach.

[23] Fredrik Westin. "Simulation of turbocharged SI-engines-with focus on the turbine". PhD thesis. Stockholm, 2005.

This page intentionally left blank.

A

Appendix A. Engine Data Tables

A.1 Final models

Baseline					
Wot					
Rpm	Torque [Nm]	Power [kW]	BSFC [g/kwh]	Boost [bar]	Inj Duration [s]
1000	88.5	9.3	260.4	1.15	0.000936
2000	113.8	23.8	239.1	1.39	0.001106
3000	125.1	39.3	241.9	1.55	0.001234
4000	117.4	49.2	255.8	1.73	0.001229
5000	102.4	53.6	275.6	1.88	0.001207
6000	82.6	51.9	311.8	1.95	0.001042

Figure A.1: Final Baseline engine

Olshammar with sideport					
Wot					
Rpm	Torque [Nm]	Power [kW]	BSFC [g/kwh]	Boost [bar]	Inj Duration [s]
1000	89	9.3	262.7	1.17	0.000952
2000	115	24.1	235.2	1.36	0.001102
3000	125.3	39.4	232	1.51	0.001183
4000	117.3	49.1	246.4	1.64	0.001178
5000	102.6	53.7	272	1.81	0.001135
6000	82.2	51.6	320.5	1.96	0.001082

Figure A.2: Final Olshammar engine with sideport

Olshammar without sideport				
Wot				
Rpm	Torque [Nm]	Power [kW]	BSFC [g/kwh]	Boost [bar]
1000	88.6	9.3	263.5	1.17
2000	114.9	24.1	236	1.38
3000	124.4	39.1	233.1	1.49
4000	116.8	48.9	248.4	1.65
5000	103.2	54	275.6	1.85
6000	81.2	51	328.1	2

Figure A.3: Final Olshammar engine without sideport

A.2 Timestep analysis

Olshammar	sideport off				
Timestep	Tolereance	RPM	Torque	Power	BSFC
t = 2 sec					
T/100	0.01	3000	112.2	35.3	254.1
T/250	0.001	3000	122.3	38.4	236.3
T/500	0.001	3000	122.3	38.4	236.3
T/1000	0.01	3000	122.3	38.4	236.5
T/5000	0.01	3000	122.3	38.4	236.5
T/10000	0.01	3000	122.3	38.4	236.5
t = 3.5 sec					
T/100	0.01	3000	112.2	35.2	254
T/100	0.001	3000	123.5	38.8	234.7
T/100	0.0001	3000	124.4	39.1	233.1
T/100	0.00001	3000	124.2	39	233.6
T/250	0.01	3000	112.2	35.3	254.1
T/250	0.001	3000	123.5	38.8	234.6
T/250	0.0001	3000	124.2	39	233.6
T/250	0.00001	3000	124.2	39	233.6
T/500	0.01	3000	112.2	35.3	254.1
T/500	0.001	3000	123.5	38.8	234.6
T/500	0.0001	3000	124.2	39	233.6
T/500	0.00001	3000	124.2	39	233.6
T/1000	0.01	3000	112.2	35.3	254.1
T/1000	0.001	3000	123.5	38.8	234.6
T/1000	0.0001	3000	124.2	39	233.6
T/1000	0.00001	3000	124.2	39	233.6
T/5000	0.01	3000	112.2	35.3	254.1
T/5000	0.001	3000	123.5	38.8	234.6
T/5000	0.0001	3000	124.2	39	233.6
T/5000	0.00001	3000	124.2	39	233.6

Figure A.4: Timestep analysis

A.3 Spark timing sweep

Olshammar without sideport							
Rpm	Spark ATDC [CAD]	Torque [Nm]	Power [kW]	BSFC [g/kwh]	Boost [bar]	Max pressure [bar]	BMF knock
1000	5	82	8.6	284.4	1.14	40.8	0.88
1000	0	84.9	8.9	273.3	1.14	46.9	0.75
1000	-5	86.6	9.1	266.3	1.14	53.7	0.69
1000	-10	86.6	9.1	264.3	1.14	60.9	0.68
1000	-15	84.7	8.9	268.2	1.14	68.1	0.69
1000	-20	80.7	8.4	282.2	1.14	74.6	0.72
1000	-25	74.3	7.8	303.5	1.14	79.7	0.75
1000	-30	66.6	7	335.3	1.14	83.6	0.78
1000	-35	58.2	6.1	381.7	1.14	86.3	0.81
1000	-40	49	5.2	449.8	1.14	87.9	0.85

Olshammar without sideport							
Rpm	Spark ATDC [CAD]	Torque [Nm]	Power [kW]	BSFC [g/kwh]	Boost [bar]	Max pressure [bar]	BMF knock
2000	5	106.8	22.4	253.5	1.36	50.3	0.97
2000	0	111.1	23.3	243.6	1.36	57.7	0.93
2000	-5	113.9	23.9	237.5	1.36	66	0.91
2000	-10	114.5	24	235.2	1.36	74.6	0.92
2000	-15	111.9	23.5	237.3	1.36	82.5	0.92
2000	-20	107.8	22.6	243.7	1.36	90	0.91
2000	-25	102.2	21.4	254.9	1.36	96.7	0.91
2000	-30	95.1	19.9	271.9	1.36	102.3	0.91
2000	-35	87	18.2	296.1	1.36	106.7	0.93
2000	-40	78.1	16.3	239.3	1.36	109.8	0.94

Olshammar without sideport							
Rpm	Spark ATDC [CAD]	Torque [Nm]	Power [kW]	BSFC [g/kwh]	Boost [bar]	Max pressure [bar]	BMF knock
3000	5	116.4	36.6	252.9	1.51	55.4	0
3000	0	121.3	38.1	242.2	1.51	63.6	1
3000	-5	125	39.3	234.9	1.51	72.8	1
3000	-10	125.2	39.4	231.8	1.51	81.7	0.99
3000	-15	123	38.7	232.4	1.51	90.4	0.98
3000	-20	119.4	37.5	236.9	1.51	98.8	0.96
3000	-25	114.2	35.9	245.4	1.51	106.4	0.93
3000	-30	107.8	33.9	259.1	1.51	113	0.92
3000	-35	100.2	31.5	277.8	1.51	118.3	0.93
3000	-40	91.7	28.8	303.7	1.51	122.5	0.94

Olshammar without sideport							
Rpm	Spark ATDC [CAD]	Torque [Nm]	Power [kW]	BSFC [g/kwh]	Boost [bar]	Max pressure [bar]	BMF knock
4000	5	105.9	44.4	273	1.64	54.9	0
4000	0	111.1	46.5	260	1.64	63.1	0
4000	-5	115	48.2	251.4	1.64	72.3	0
4000	-10	117.3	49.1	246.3	1.64	82.2	1
4000	-15	116.2	48.7	246.3	1.64	91.3	1
4000	-20	112	46.9	250.5	1.64	99.1	0.97
4000	-25	107	44.8	258.9	1.64	106.5	0.93
4000	-30	101.1	42.3	272.4	1.64	113.1	0.92
4000	-35	94.3	39.5	291.6	1.64	118.7	0.93
4000	-40	86.9	36.4	317.8	1.64	123.5	0.94

Olshammar without sideport							
Rpm	Spark ATDC [CAD]	Torque [Nm]	Power [kW]	BSFC [g/kwh]	Boost [bar]	Max pressure [bar]	BMF knock
5000	5	91.1	47.6	307	1.81	53.4	0
5000	0	96.2	50.3	290.5	1.81	61.4	0
5000	-5	100.2	52.3	279	1.81	70.4	0
5000	-10	102.5	53.6	272	1.81	80	0
5000	-15	103.3	54	270.1	1.81	89.9	0.1
5000	-20	101.7	53.1	274.4	1.81	99.1	0.94
5000	-25	96.3	50.4	283.9	1.81	105.9	0.91
5000	-30	90.8	47.5	299.1	1.81	112.4	0.9
5000	-35	85	44.4	320.7	1.81	118.5	0.91
5000	-40	78.8	41.1	350.1	1.81	124.3	0.93

Olshammar without sideport							
Rpm	Spark ATDC [CAD]	Torque [Nm]	Power [kW]	BSFC [g/kwh]	Boost [bar]	Max pressure [bar]	BMF knock
6000	5	70.7	44.6	371.3	1.96	50.9	0
6000	0	75.7	47.6	346.6	1.96	58.5	0
6000	-5	79.5	50.1	329.9	1.96	67.1	0
6000	-10	81.9	51.7	319.5	1.96	76.3	1
6000	-15	82.8	52.2	315.9	1.96	85.7	0.95
6000	-20	82	51.6	319.1	1.96	94.9	0.88
6000	-25	79.4	50	329.3	1.96	103.2	0.85
6000	-30	75.2	47.3	348.5	1.96	110.3	0.85
6000	-35	69.4	43.7	376.7	1.96	116.1	0.87
6000	-40	62.5	39.4	418.1	1.96	120.6	0.9

Figure A.5: Spark ignition timing sweep for the Olshammar engine. Each table is for one engine speed.

Baseline							
Rpm	Spark ATDC [CAD]	Torque [Nm]	Power [kW]	BSFC [g/kwh]	Boost [bar]	Max pressure [bar]	BMF knock
1000	5	84.3	8.8	270.7	1.15	41.4	0.85
1000	0	87.5	9.2	260.1	1.15	47.7	0.74
1000	-5	89.3	9.3	256.2	1.15	54.6	0.69
1000	-10	88.4	9.3	259.9	1.15	61.4	0.68
1000	-15	85	8.9	266.3	1.14	67.6	0.7
1000	-20	79.9	8.4	279.1	1.13	73.3	0.73
1000	-25	73.5	7.7	299.7	1.12	78.1	0.76
1000	-30	66	6.9	330.7	1.11	81.9	0.79
1000	-35	57.6	6	375.6	1.11	84.4	0.82
1000	-40	48.8	5.1	441.2	1.1	86	0.85

Baseline							
Rpm	Spark ATDC [CAD]	Torque [Nm]	Power [kW]	BSFC [g/kwh]	Boost [bar]	Max pressure [bar]	BMF knock
2000	5	105.3	22	258.9	1.36	50.7	0.97
2000	0	109.6	23	248.6	1.36	58.2	0.93
2000	-5	112.6	23.6	242.1	1.36	66.5	0.91
2000	-10	113.9	23.8	239.2	1.36	75.5	0.91
2000	-15	113.2	23.7	240.4	1.36	84.6	0.91
2000	-20	110.6	23.2	246.3	1.36	93.3	0.9
2000	-25	105.9	22.2	256.9	1.36	101.1	0.9
2000	-30	99.3	20.8	273.8	1.36	107.6	0.9
2000	-35	91.2	19.1	298	1.36	112.5	0.91
2000	-40	81.7	17.1	332.8	1.36	115.6	0.93

Baseline							
Rpm	Spark ATDC [CAD]	Torque [Nm]	Power [kW]	BSFC [g/kwh]	Boost [bar]	Max pressure [bar]	BMF knock
3000	5	114	35.8	266.9	1.56	57.2	1
3000	0	119.4	37.5	254.6	1.56	65.7	0.99
3000	-5	123.2	38.7	246.2	1.56	75.1	0.99
3000	-10	125.4	39.4	241.5	1.56	85.3	0.98
3000	-15	125.6	39.5	240.9	1.56	95.7	0.97
3000	-20	123.6	38.8	244.5	1.56	105.7	0.94
3000	-25	119.5	37.5	252.9	1.56	114.8	0.91
3000	-30	113.3	35.6	266.5	1.56	122.4	0.9
3000	-35	105.5	33.1	286.1	1.56	128.5	0.91
3000	-40	96.2	30.2	313.5	1.56	133	0.93

Baseline							
Rpm	Spark ATDC [CAD]	Torque [Nm]	Power [kW]	BSFC [g/kwh]	Boost [bar]	Max pressure [bar]	BMF knock
4000	5	105.8	44	287.6	1.72	57.4	0
4000	0	110.6	46.3	272.4	1.72	65.9	0
4000	-5	114.9	48.1	261.7	1.72	75.4	0
4000	-10	117.4	49.2	255.5	1.72	85.6	1
4000	-15	118	49.5	253.8	1.72	96	0.99
4000	-20	116.5	48.8	256.5	1.72	106	0.95
4000	-25	113.1	47.4	264.2	1.72	115.3	0.91
4000	-30	107.6	45	277.5	1.72	123.1	0.9
4000	-35	100.3	42	297.6	1.72	129.4	0.91
4000	-40	91.8	38.5	325.2	1.72	134.2	0.93

Baseline							
Rpm	Spark ATDC [CAD]	Torque [Nm]	Power [kW]	BSFC [g/kwh]	Boost [bar]	Max pressure [bar]	BMF knock
5000	5	90.2	47.2	314.6	1.87	54.5	0
5000	0	95.7	50	296.1	1.87	62.6	0
5000	-5	99.7	52.2	282.6	1.87	71.7	0
5000	-10	102.5	53.7	274.8	1.87	81.4	1
5000	-15	103.5	54.2	271.9	1.87	91.4	0.99
5000	-20	102.5	53.7	273.9	1.87	101.1	0.92
5000	-25	99.6	52.1	282.2	1.87	109.9	0.88
5000	-30	95	49.6	295.9	1.87	117.5	0.88
5000	-35	88.5	46.3	317.5	1.87	123.6	0.89
5000	-40	80.9	42.3	347.8	1.87	128.2	0.91

Baseline							
Rpm	Spark ATDC [CAD]	Torque [Nm]	Power [kW]	BSFC [g/kwh]	Boost [bar]	Max pressure [bar]	BMF knock
6000	5	70.3	44.3	365.4	1.93	50	0
6000	0	75.5	47.5	340.7	1.93	57.5	0
6000	-5	79.8	50.1	322.5	1.93	65.9	0
6000	-10	82.6	51.9	311.4	1.93	74.9	1
6000	-15	83.8	52.7	306.3	1.93	84.2	0.94
6000	-20	83.1	52.2	308.9	1.93	93.1	0.87
6000	-25	80.7	50.7	318.1	1.93	101.3	0.85
6000	-30	76.5	48.1	335.3	1.93	108.3	0.85
6000	-35	70.9	44.6	361.9	1.93	114	0.87
6000	-40	64	40.2	400.9	1.93	118.3	0.9

Figure A.6: Spark ignition timing sweep for the Baseline engine. Each table is for one engine speed.

A.4 Exhaust Cylinder Offset

Exhaust Offset				
rpm	exh offset	torque	power	bsfc
2000	-20	100.4	21	237.8
2000	-15	103.3	21.6	237
2000	-10	106.4	22.3	236.6
2000	-5	110.1	23.1	235.8
2000	0	114.2	23.9	235.3
2000	5	114.7	24	236.1
2000	10	114	23.9	237.7
2000	15	113.3	23.7	239.4
2000	20	112.4	23.6	241.2
4000	-20	107.9	45.1	255
4000	-15	110.3	46.2	252.5
4000	-10	112.6	47.1	250.2
4000	-5	114.9	48.1	248.3
4000	0	117.4	49.1	246.3
4000	5	117.9	49.3	245.6
4000	10	118.1	49.4	245.4
4000	15	118.1	49.5	245.7
4000	20	117.9	49.4	246.5
6000	-20	78	49	336.5
6000	-15	79.3	49.7	331.6
6000	-10	80.3	50.4	327.1
6000	-5	81.1	51	323
6000	0	82.2	51.5	319.5
6000	5	82.7	51.9	316.5
6000	10	83.3	52.3	314
6000	15	83.8	52.6	312.2
6000	20	84.3	52.8	310.6

Figure A.7: Variation of exhaust cylinder offset for 2000-6000 rpm.

A.5 Bore and stroke variation

Olshammar		Exhaust cylinder sideport					
Wot							
Rpm	Bore	Stroke	Torque [Nm]	Power [kW]	BSFC [g/kwh]	Boost [bar]	
2000	40	100	113.2		238.8	1.36	
2000	60	100	113.7		237.8	1.36	
2000	80	100	110.7		236.4	1.36	
2000	100	100	110.3		235.7	1.36	
2000	110	90	111.8		235.6	1.36	
2000	110	100	111.6		235.6	1.36	
2000	110	110	111.5		235.6	1.36	heatmap new
2000	110	120	111.4		235.6	1.36	
2000	120	90	115.1		234.9	1.36	
2000	120	100	115		235.3	1.36	
2000	120	110	114.8		235.3	1.36	
2000	120	120	114.7		235.3	1.36	
2000	130	90	114.2		237	1.36	
2000	130	100	114.2		236.8	1.36	
2000	130	110	114.3		236.8	1.36	
2000	130	120	114.3		236.7	1.36	
2000	120	40	115		235.2		
2000	120	70	115.1		235.1		
2000	120	100	115		235.4		
2000	120	130	114.5		235.4		
2000	150	40	110.5		245.6		
2000	150	70	110.7		245		
2000	150	100	111		244.5		
2000	150	130	111.3		243.9		
2000	180	40	101.6		268.4		
2000	180	70	102.3		266.8		
2000	180	100	102.9		265.3		
2000	180	130	103.5		263.8		
3000	110	90	120.6		233.2		
3000	110	100	120.2		233.3		
3000	110	110	119.8		233.4		
3000	110	120	119.4		233.5		
3000	120	90	125.7		231.7		
3000	120	100	125.2		231.8		heatmap new
3000	120	110	124.8		232		
3000	120	120	124.3		232		
3000	130	90	126.7		232.4		
3000	130	100	126.7		232.1		
3000	130	110	126.8		232.2		
3000	130	120	126.9		232		

Figure A.8: Bore and stroke variation.

B

Appendix B. Exhaust Pulse Effects on Compressor and Turbine Efficiency

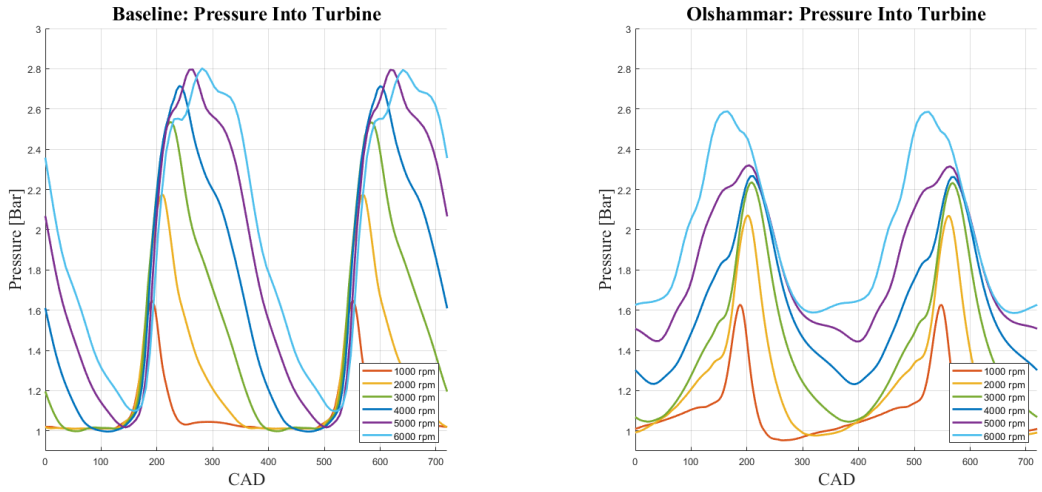

Figure B.1: Comparison of pressure into turbine.

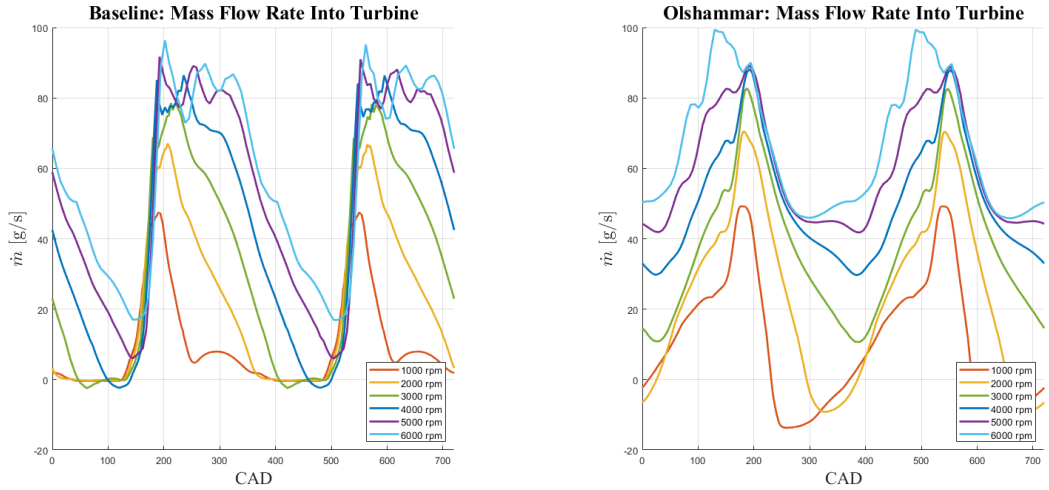

Figure B.2: Comparison of mass flow rate into turbine.

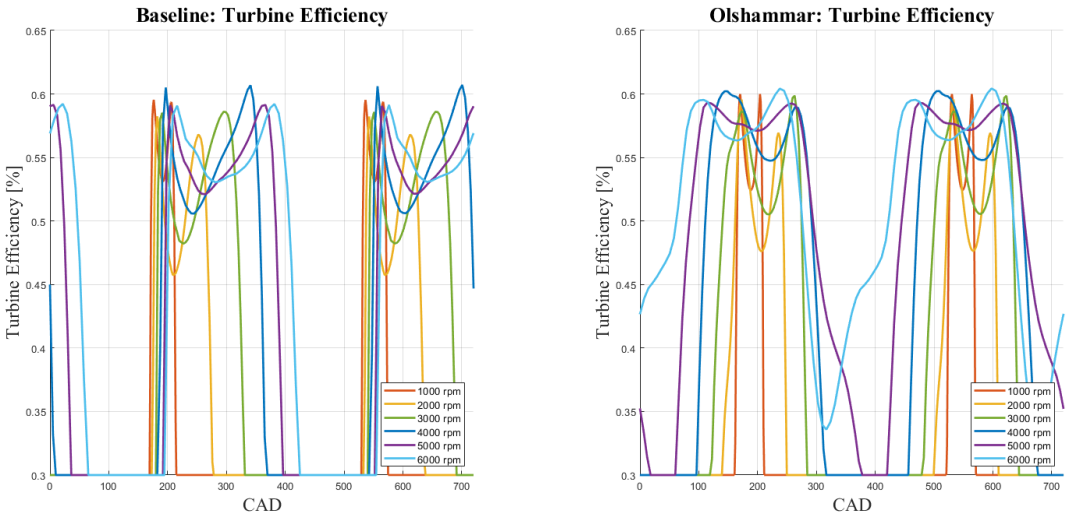

Figure B.3: Comparison of turbine efficiency.

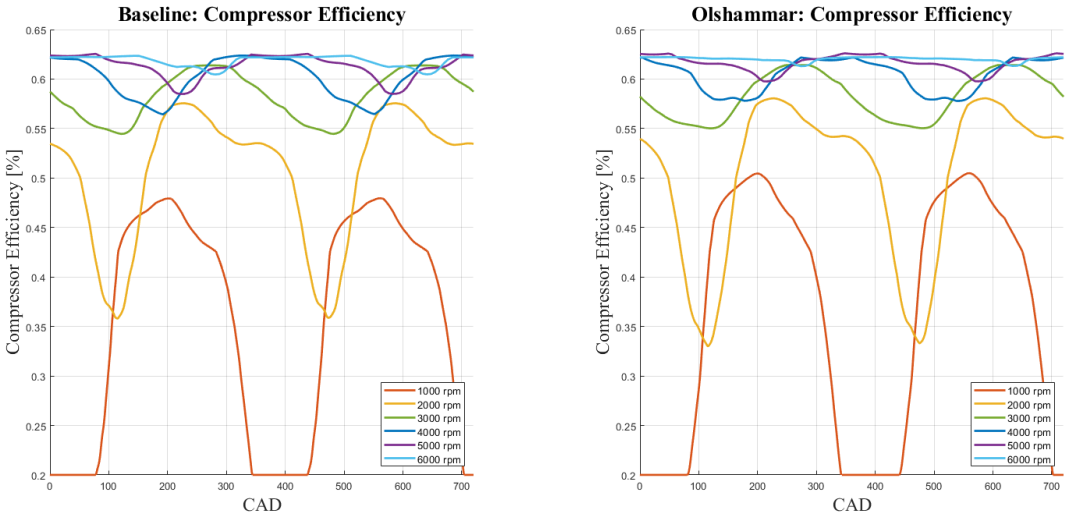

Figure B.4: Comparison of compressor efficiency

DEPARTMENT OF MECHANICS AND MARITIME SCIENCES
CHALMERS UNIVERSITY OF TECHNOLOGY
Gothenburg, Sweden
www.chalmers.se

CHALMERS
UNIVERSITY OF TECHNOLOGY